

# Evidence for a SAL1-PAP Chloroplast Retrograde Pathway That Functions in Drought and High Light Signaling in *Arabidopsis*

Gonzalo M. Estavillo,<sup>a</sup> Peter A. Crisp,<sup>a</sup> Wannarat Pornsiriwong,<sup>a</sup> Markus Wirtz,<sup>b</sup> Derek Collinge,<sup>a</sup> Chris Carrie,<sup>c</sup> Estelle Giraud,<sup>c</sup> James Whelan,<sup>c</sup> Pascale David,<sup>d</sup> H el ene Javot,<sup>d</sup> Charles Brearley,<sup>e</sup> R udiger Hell,<sup>b</sup> Elena Marin,<sup>d</sup> and Barry J. Pogson<sup>a,1</sup>

<sup>a</sup> Australian Research Council Centre of Excellence in Plant Energy Biology, Research School of Biology, Australian National University Canberra, Acton, Australian Capital Territory 0200, Australia

<sup>b</sup> University of Heidelberg, Heidelberg Institute for Plant Sciences, 69120 Heidelberg, Germany

<sup>c</sup> ARC Centre of Excellence in Plant Energy Biology, University of Western Australia, Crawley, Western Australia 6009, Australia

<sup>d</sup> Commissariat   l'Energie Atomique, Direction des Sciences du Vivant Institut de Biologie Environnementale et de Biotechnologie, Laboratoire de Biologie du D veloppement des Plantes, Unit  Mixte de Recherche 6191 Centre National de la Recherche Scientifique, Commissariat   l'Energie Atomique, Aix-Marseille II, F-13108 Saint-Paul-lez-Durance, France

<sup>e</sup> School of Biological Sciences, University of East Anglia, Norwich NR4 7TJ, United Kingdom

**Compartmentation of the eukaryotic cell requires a complex set of subcellular messages, including multiple retrograde signals from the chloroplast and mitochondria to the nucleus, to regulate gene expression. Here, we propose that one such signal is a phosphonucleotide (3'-phosphoadenosine 5'-phosphate [PAP]), which accumulates in *Arabidopsis thaliana* in response to drought and high light (HL) stress and that the enzyme SAL1 regulates its levels by dephosphorylating PAP to AMP. SAL1 accumulates in chloroplasts and mitochondria but not in the cytosol. *sal1* mutants accumulate 20-fold more PAP without a marked change in inositol phosphate levels, demonstrating that PAP is a primary *in vivo* substrate. Significantly, transgenic targeting of SAL1 to either the nucleus or chloroplast of *sal1* mutants lowers the total PAP levels and expression of the HL-inducible *ASCORBATE PEROXIDASE2* gene. This indicates that PAP must be able to move between cellular compartments. The mode of action for PAP could be inhibition of 5' to 3' exoribonucleases (XRNs), as SAL1 and the nuclear XRNs modulate the expression of a similar subset of HL and drought-inducible genes, *sal1* mutants accumulate XRN substrates, and PAP can inhibit yeast (*Saccharomyces cerevisiae*) XRNs. We propose a SAL1-PAP retrograde pathway that can alter nuclear gene expression during HL and drought stress.**

## INTRODUCTION

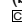
The evolution of the eukaryotic cell necessitated the development of signaling between compartments or organelles to coordinate cell differentiation, development, and acclimation to altered environmental stimuli. In plants, the transcriptional and developmental program of the chloroplast is tightly integrated with the nuclear program (Vranov a et al., 2002; Nott et al., 2006; Pogson et al., 2008; Kleine et al., 2009; Pfannschmidt, 2010). This is required because chloroplast multiprotein complexes, such as ribosomes and the photosystems, are mosaics of subunits transcribed from both the plastid and nuclear genomes. Thus,

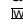
coexpression from both genomes is essential to enable coordinated assembly and maintenance of photosynthesis. For example, if chloroplasts become damaged, they initiate retrograde signals that are sent to the nucleus to preclude unnecessary transcription of nuclear-encoded proteins that are targeted to the chloroplast (Bradbeer et al., 1979). A range of signals and pathways have been proposed and actively debated (Pogson et al., 2008; Kleine et al., 2009; Pfannschmidt, 2010). However, no chemical signal has been reported that moves directly from the chloroplast to the nucleus via the cytosol to regulate gene expression nor has a protein been reported that directly regulates the levels of such a compound.

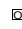
There is evidence for multiple retrograde pathways; indeed, given the complexity and number of different metabolic reactions undertaken within the plastid, that is to be expected (Pogson et al., 2008; Pfannschmidt, 2010). Retrograde signals can be divided into two classes: those related to chloroplast and photosystem biogenesis (biogenic control) and those related to the operation of the chloroplast in response to changing environmental stimuli (operational control) (Pogson et al., 2008). Forward genetic screens have identified several protein components of biogenic control signaling pathways. Examples of biogenic

<sup>1</sup> Address correspondence to barry.pogson@anu.edu.au.

The author responsible for distribution of materials integral to the findings presented in this article in accordance with the policy described in the Instructions for Authors (www.plantcell.org) is: Barry J. Pogson (barry.pogson@anu.edu.au).

 Some figures in this article are displayed in color online but in black and white in the print edition.

 Online version contains Web-only data.

 Open Access articles can be viewed online without a subscription. www.plantcell.org/cgi/doi/10.1105/tpc.111.091033

control mutants include the *snowy cotyledon* (Albrecht et al., 2010) and *genomes uncoupled (gun)* mutants (Susek et al., 1993; Larkin et al., 2003; Strand et al., 2003; Koussevitzky et al., 2007; Ruckle et al., 2007). With respect to biogenic control, a tetrapyrrole was proposed to move from the chloroplast to cytosol where it was hypothesized it would interact with cytosolic targets such as HSP90 (Strand et al., 2003; Kindgren et al., 2011). However, this has been actively debated by other groups (Mochizuki et al., 2008; Moulin et al., 2008). Recently, another tetrapyrrole, heme, was proposed as a putative plastid biogenic signal in plants, but no changes in heme levels or evidence for heme movement from the chloroplast were reported nor were cytosolic/nuclear signaling partners described (Woodson et al., 2011). Although there is evidence that tetrapyrroles trigger retrograde signaling in plants, what the actual pathways are remains an open question (Pfannschmidt, 2010).

With respect to operational control or chloroplast-nuclear signaling in response to environmental stimuli, considerable detail is understood about the initiation of signaling cascades in the chloroplast and transcriptional changes in the nucleus, but the intervening steps are largely unknown. Environmental stresses that perturb photosynthesis, such as high light (HL) and drought, induce reactive oxygen species (ROS), changes in redox state of plastoquinone, and changes in abscisic acid (ABA) concentration that are implicated in the HL response pathways (Karpinski et al., 1999; Vranová et al., 2002; Nott et al., 2006; Rossel et al., 2006; Lee et al., 2007; Pogson et al., 2008; Van Breusegem et al., 2008; Foyer and Noctor, 2009; Galvez-Valdivieso et al., 2009; Kleine et al., 2009; Pfannschmidt et al., 2009; Wilson et al., 2009). In the nucleus, HL alters the expression of ~700 genes (Rossel et al., 2007), including *APX2* (Karpinski et al., 1999; Rossel et al., 2006) and *EARLY LIGHT INDUCIBLE PROTEIN2 (ELIP2)* (Harari-Steinberg et al., 2001; Kimura et al., 2003). A number of transcription factors are induced by HL, including DROUGHT RESPONSE BINDING 2A (*DREB2A*) and *ZAT10*; the latter can regulate the expression of 18% of the HL transcriptome, including *APX2* (Rossel et al., 2007). Other HL-inducible genes, such as *ELIP2*, are regulated by cryptochromes (Kleine et al., 2007).

To identify steps between initiation of the signal and perception in the nucleus, screens for altered gene expression during oxidative stress have identified a series of mutations, including *executer1* and 2, *regulator of APX2*, and *altered APX2 expression8 (alx8)* (Ball et al., 2004; Wagner et al., 2004; Rossel et al., 2006; Wilson et al., 2009). Yet, the actual retrograde signals regulated by the multiple biogenic and operational pathways still remain unknown.

The *alx8* mutant exhibits constitutive upregulation of 25% of the HL-regulated transcriptome, including *ZAT10*, *DREB2A*, *ELIP2*, and *APX2*, along with hyperexpression of these transcripts upon HL stress (Rossel et al., 2006; Wilson et al., 2009). Indeed, as 70% of HL-inducible genes are also upregulated by drought (Kimura et al., 2002), it was not surprising that the *alx8* mutant is also drought tolerant, surviving water deprivation up to 50% longer than wild-type plants. These phenotypes are caused by a lesion in the *SAL1/ALX8/FRY1* gene and implicate SAL1 as a component of HL and drought stress signaling networks (Wilson et al., 2009; Hirsch et al., 2011).

SAL1 is a phosphatase that hydrolyzes a phosphate group from both phosphonucleotides and inositol polyphosphates in vitro (Quintero et al., 1996; Xiong et al., 2001). Inositol 1,4,5-trisphosphate (IP<sub>3</sub>) is viewed as one of the most logical targets for SAL1 in vivo (Xiong et al., 2001; Zhang et al., 2011). However, other findings using mutants and transgenic plants suggest SAL1 may be degrading 3'-phosphoadenosine 5'-phosphosulfate (PAPS) (Rodríguez et al., 2010) or 3'-phosphoadenosine 5'-phosphate (PAP) (Gy et al., 2007; Kim and von Arnim, 2009). Moreover, the enzymatic activity of recombinant SAL1 is similar for both phosphoadenosines (Gil-Mascarell et al., 1999), but the phosphatase activity against IP<sub>3</sub> is only 4% of that against PAP (Xiong et al., 2001). The in vivo substrate is not resolved, as a recent article proposed for IP<sub>3</sub> (Zhang et al., 2011). SAL1 is involved in many cellular processes, and identification of its primary substrates is required to better understand the mode of action of this phosphatase.

PAP is produced from PAPS during sulphation reactions catalyzed by cytosolic sulfotransferases (Klein and Papenbrock, 2004). Although PAP was originally viewed as a byproduct with no physiological function in plants, it can inhibit the activity of the two yeast (*Saccharomyces cerevisiae*) 5' to 3' exoribonucleases (XRNs), thereby altering RNA catabolism (Dichtl et al., 1997). Treatment of yeast with lithium (Li<sup>+</sup>), a strong inhibitor of the yeast SAL1 homolog (Sc-SAL1), results in an increase in PAP (Murguía et al., 1996) sufficient to inhibit XRNs, resulting in the accumulation of transcripts targeted by Xrn1 in yeast (Dichtl et al., 1997; van Dijk et al., 2011). Moreover, a PAP concentration of 0.1 mM inhibits the in vitro activity of the two yeast XRNs by 40 to 65% (Dichtl et al., 1997). SAL1 has recently been linked to several developmental and morphological processes in plants (Wilson et al., 2009; Robles et al., 2010; Rodríguez et al., 2010; Zhang et al., 2011); interestingly, *Arabidopsis thaliana xrn* mutants have a similar leaf and root morphology to that of *sal1* mutants (Gy et al., 2007; Hirsch et al., 2011).

Although SAL1 functions in stress signaling and other fundamental plant processes, the subcellular localization, the in vivo substrate, and the mode of action of SAL1 are either unknown or debated. For example, the SAL1 protein has been reported to be localized in the chloroplast (Rodríguez et al., 2010), cytosol (Zhang et al., 2011), and nucleus (Kim and von Arnim, 2009) by different techniques. Consequently, it is critical to resolve its cellular location, to identify the in vivo substrates, and to investigate how the accumulation of its substrates in the cell might function in cellular signaling. More significantly, there is no indication in the literature whether PAP could act as a retrograde signal linking organelle status with nuclear gene expression. Indeed, there is no report of PAP measurements in plants, which precluded the study of its role in planta.

In this study, we show that SAL1 accumulates in both the chloroplasts and the mitochondria and provide evidence that PAP levels are modulated by SAL1. We propose that PAP functions as a mobile signal that alters RNA metabolism by inhibiting XRNs to affect stress and developmental gene expression and that the chloroplastic SAL1 protein can prevent its action by degrading PAP in the chloroplastic compartment.

## RESULTS

**SAL1 Expression Correlates Spatially with Responses to HL Stress**

We previously showed that the lack of the SAL1 protein in the *alx8* mutant promotes constitutive *APX2:LUCIFERASE* (*LUC*) expression in the vascular tissue (Rossel et al., 2006; Wilson et al., 2009). Here, we investigated the expression pattern of *SAL1* in mature leaf tissue by reporter gene analyses. Expression of green fluorescent protein (GFP) driven by the *SAL1* promoter (pSAL1:SAL1:GFP) was stronger in the vascular tissue than in the mesophyll tissue of the leaf (Figure 1A). The vascular tissue is the primary site of production of  $H_2O_2$ , especially after HL stress (Fryer et al., 2003) (Figure 1B). By contrast, the HL induction of  $H_2O_2$  in *alx8* vascular tissue was much lower, and the total  $H_2O_2$  foliar level of plants grown under normal conditions was half of that in the wild type (Figure 1C). Thus, *SAL1* expression colocalizes with *APX2:LUC* activity, with the loss of *SAL1* leading to increased *APX2* expression (Rossel et al., 2006; Wilson et al., 2009) and reduced  $H_2O_2$  levels in the vasculature. Furthermore, it demonstrates that the elevated expression of *APX2* and other HL-regulated genes is not due to elevated levels of  $H_2O_2$ .

**PAP Accumulates in *sal1* Mutants and during Drought Stress**

In vitro, SAL1 has a dual phosphatase activity against both polyphosphoinositols, such as  $IP_3$  (Xiong et al., 2001; Zhang et al., 2011), and 3'(2'),5'-biphosphate nucleotides, such as PAP or PAPS (Quintero et al., 1996). PAPS and  $IP_3$  have been reported to be in vivo substrates (Xiong et al., 2001; Rodríguez et al., 2010; Zhang et al., 2011); PAP has been suggested as a substrate based on work with transgenic plants (Kim and von Arnim, 2009; Chen and Xiong, 2010; Hirsch et al., 2011). We used two different approaches to investigate if the SAL1 phosphatase activity against PAP regulated the expression of *APX2* and, thus, ROS levels. First, we tested the hypothesis that accumulation of PAP could upregulate the *APX2* promoter and induce the *alx8* phenotype by feeding PAP to Columbia-0 (Col-0) plants transformed with the reporter gene *APX2:LUC*. However, no significant change in *APX2:LUC* activity was observed when feeding increasing concentrations of PAP to 7-d-old plants via the roots under either low light (LL) or HL (see Supplemental Figure 1 online). Failed root substrate uptake or impaired vasculature transport, import into leaf cells, or perception are possible explanations for the negative results of the feeding experiment.

Next, we directly measured inositol phosphates (IPs) in the *sal1* mutants *alx8*, *fry1-6*, and *fry1-1*. The *alx8* mutant harbors a point

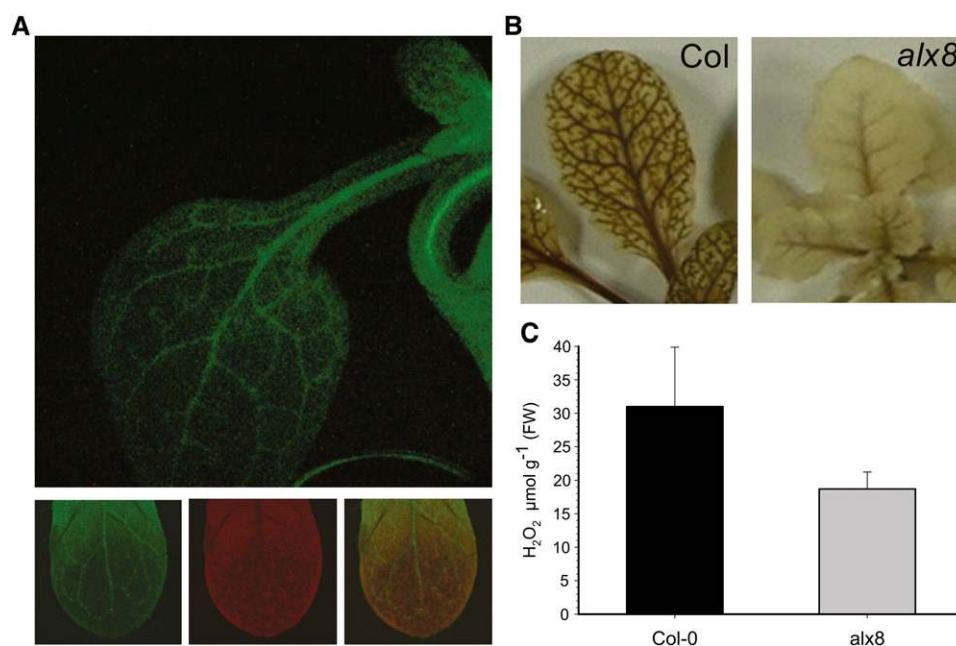


**Figure 1.** SAL1 Colocalizes in the Vascular Tissue with  $H_2O_2$ .

**(A)** Stable expression of the SAL1-GFP fusion protein in *Arabidopsis* plants. Gene expression was driven by a genomic sequence containing the endogenous *SAL1* promoter, which was fused to GFP (pSAL1:SAL1:GFP). Top panel: 8-d leaf showing a strong GFP signal in the vascular tissue and a more moderate one in the mesophyll tissues. The bottom left image is GFP channel, middle image is chlorophyll channel, and right image shows the overlay from a 2-week-old leaf.

**(B)** Visualization of  $H_2O_2$  in Col-0 and *alx8* leaves after 1 h HL treatment using DAB.  $H_2O_2$  accumulation is visualized as a dark, brown precipitate.

**(C)** Quantification of leaf  $H_2O_2$  in 6-week-old, soil-grown Col-0 and *alx8*. After extraction and incubation with the Amplex Red, the amount of  $H_2O_2$  was quantified against a standard curve and normalized to the FW. The mean and SD are shown. Asterisk indicates significant difference relative to Col-0 (*t* test,  $P < 0.05$ ,  $n = 5$ ).

mutation in *SAL1* that renders the recombinant protein enzymatically inactive (Wilson et al., 2009), whereas the *fry1-6* allele is a T-DNA insertion mutant (SALK\_020882). Both mutants, in the Col-0 background, lacked detectable SAL1 protein and showed very similar rosette morphology (see Supplemental Figure 2 online). The third mutant, *fry1-1*, previously described in the C24 background, was reported to have increased IP<sub>3</sub> (Xiong et al., 2001), and increased IP<sub>3</sub> by 1.5- to 2.0-fold was recently reported in another *sal1* mutant (Zhang et al., 2011), as measured by displacement bioassays. It was not revealed whether other IP compounds could be affected. To test this, we grew young seedlings in the presence of radiolabeled *myo*-[2-<sup>3</sup>H]inositol and showed that all the IP pools were similar in Col-0, *alx8*, *fry1-6* (Figures 2A to 2C), and *fry1-1* (see Supplemental Figure 3 online).

Finally, we investigated whether PAP, or PAPS, is the *in vivo* substrate of SAL1 and developed a highly sensitive and specific fluorescence labeling-based HPLC method for quantification of

these nucleotides (Figure 2D; see Supplemental Figure 4 online). Using this technique, we could clearly quantify PAP and PAPS based on the chromatograms of plant extracts with adenosines derivatized to enable their detection by fluorescence spectroscopy. We found that PAP accumulated 20-fold in three *sal1* mutants, *alx8* (Table 1), *fry1-6*, and *fou8* (see Supplemental Figure 5 online), compared with wild-type plants. There was also a significant but minor increase in PAPS in *alx8* and no significant changes in adenosine 5'-phosphosulfate (APS), the sole precursor of PAPS, and an intermediate in the synthesis of Cys. Nor was there any change in GSH, the storage form of Cys. The specific and substantial increase of PAP in *sal1* mutants provides the first direct evidence that SAL1 has *in vivo* nucleotidase activity preferentially against PAP.

The correlation between higher PAP levels in *alx8* and drought tolerance led us to investigate a role for this metabolite during abiotic stress responses. Thus, we analyzed PAP levels

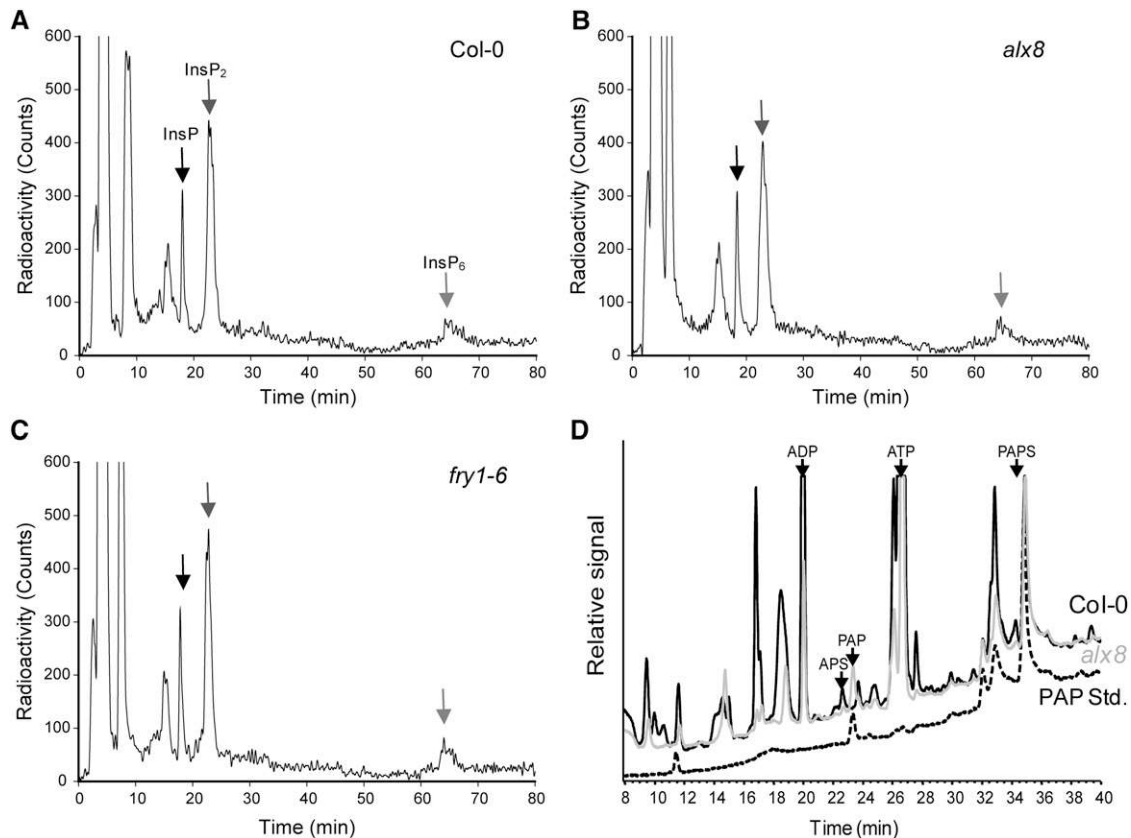


**Figure 2.** PAP, and Not IPs, Accumulates in *alx8*.

(A) to (C) Analyses of phosphoinositols in different genotypes. Five to six 10-d-old Col-0 (A), *alx8* (B), or *fry1-6* (C) seedlings were labeled with *myo*-[2-<sup>3</sup>H]inositol for 72 h and IPs extracted in HCl prior to separation by HPLC. Chromatograms show representative profile of phosphoinositols of one of two independent experiments. The intensity and periodicity of the peaks corresponding to inositol mono-, bis-, and hexakisphosphate (arrows) are similar in all genotypes.

(D) Isolation and identification of phosphoadenosine nucleotides. Metabolites were extracted from leaves of 30-d-old plants and adenosines fluorescently labeled by derivatization. PAPS, APS, and PAP in wild-type Col-0 (black) and *alx8* (gray) were identified by coelution with external PAP standard (dashed black line). A typical chromatogram is shown. Note that approximately fourfold less extract of *alx8* than Col-0 was injected in this experiment. Quantification was undertaken using a standard curve (see Supplemental Figure 4 online).

**Table 1.** Quantification of Nucleotide Phosphates and Glutathione-Related Metabolites

Germplasm	PAP Metabolism			Glutathione Metabolism		
	APS	PAPS	PAP	Cys	$\gamma$ -EC	GSH
Col-0	4.2 $\pm$ 1.4	1.1 $\pm$ 0.1	0.6 $\pm$ 0.2	4.8 $\pm$ 1.0	2.7 $\pm$ 0.6	176 $\pm$ 48
<i>alx8</i>	3.8 $\pm$ 0.2	1.8 $\pm$ 0.1	11.8 $\pm$ 1.4	8.1 $\pm$ 3.4	4.5 $\pm$ 1.6	197 $\pm$ 62
	ns	P < 10 <sup>-4</sup>	P < 10 <sup>-4</sup>	P < 0.05	P < 0.05	ns

Metabolite concentrations were determined by HPLC for 30-d-old plants.  $\gamma$ -EC, L- $\gamma$ -glutamylcysteine. Values are the concentration in pmol/mg FW  $\pm$  SD ( $n = 4$ ). Individual P numbers compared to Col-0 after *t* test analyses assuming two-tailed and two-sample unequal variance are indicated. ns, not significant.

in response to drought and HL in wild-type plants. PAP levels increased 30-fold in leaves of drought-stressed wild-type plants, coincident with a substantial decrease in plant relative water content (RWC) after 7 to 11 d of drought (Figure 3). Analysis of variance (ANOVA) two-factor analyses indicated strong interaction between day and genotype for RWC and PAP, being significantly higher for *alx8* relative to Col-0 ( $P < 0.001$ ). This increase did not occur in the early phase of drought and was observed only when there was a decline in RWC. A similar trend was observed for *alx8*, but it was delayed, again with PAP only rising as RWC declined. Similarly, exposure of Col-0 plants to HL for just 1 h resulted in significantly ( $P < 0.005$ ) higher PAP levels than in plants kept at LL (0.9  $\pm$  0.2 versus 0.6  $\pm$  0.2 pmol of PAP/mg fresh weight [FW], respectively), although this increase was much smaller than that observed during drought. Taken together, these results revealed that the level of the sulfur-related metabolite PAP was elevated in mutants lacking SAL1 and increased in response to at least two abiotic stresses.

### SAL1 Localizes to Both Chloroplast and Mitochondria

Contrasting results have been obtained regarding the cellular localization of SAL1 (Kim and von Arnim, 2009; Rodríguez et al., 2010; Zhang et al., 2011). To resolve this debate, we used three different methods to investigate SAL1 location. First, a full-length SAL1 fused at the C terminus to GFP accumulated in both chloroplasts and mitochondria of transiently transformed *Arabidopsis* cells (Figure 4A). The chloroplasts and mitochondria were visualized by red fluorescent protein (RFP) fused to either the small subunit (SSU) of ribulose-1,5-bis-phosphate carboxylase/oxygenase (Rubisco) transit peptide or to the targeting domain of the ALTERNATIVE OXIDASE1 (AOX1), respectively. Second, to verify that this expression pattern was not an artifact due to the use of transitory expression systems, we generated stable transgenic lines. SAL1:GFP fusion protein driven by the native promoter showed SAL1 in both organelles in mesophyll protoplasts isolated from stably transformed pSAL1:SAL1:GFP plants (Figure 4B). The chloroplasts were visualized by chlorophyll fluorescence and the mitochondria by MitoRed. Effectively all compartmentalized GFP could be attributed to either mitochondria or chloroplasts, not nuclei. Third, we developed a new chloroplast and cytosolic fractionation method (see Supplemental Figure 6 online and Methods) that allowed us to detect SAL1 unequivocally as an ~38-kD band in purified chloroplast and mitochondria fractions of Col-0 leaves by immunological

methods (Figure 4C). The molecular mass of this band matches that of the recombinant protein lacking the deduced 54-amino acid chloroplast transit peptide (Wilson et al., 2009). The relative purity of the fractions was demonstrated by probing with antibodies against chloroplastic Lhcb, mitochondrial TOM40, and cytosolic UGPase. UGPase was enriched in the cytosolic fraction, and although there was a band in the chloroplast fraction, it is of lower molecular mass than UGPase, and as it is the same size as Rubisco, it is likely that this is a cross-reaction to Rubisco. Significantly, neither Lhcb, TOM40, nor the unprocessed or mature forms of SAL1 were detected in the cytosolic fraction.

We attempted to assay PAP from the cytosolic fractions used for the protein purification, but we observed that PAP is labile in tissue extracts, and as a consequence, it was not detected after the lengthy purification procedure. However, analyses of phosphonucleotides from Col-0 chloroplasts prepared by a different, more rapid protocol identified a peak that matched that of the PAP standard, suggesting that PAP is present in the chloroplasts of *Arabidopsis* (Figure 4D). All this evidence supports the conclusion that SAL1 accumulates in mitochondria and chloroplasts and that PAP can be detected in chloroplasts.

### Complementation of *sal1* Mutants Demonstrates That PAP Regulates Nuclear Gene Expression

Having demonstrated that SAL1 is required for the catabolism of PAP, we sought to investigate whether PAP could act as a mobile signal within the cell, capable of entering the nucleus and regulating gene expression. Due to the aforementioned technical difficulties of measuring adenosines in different cellular compartments, we used a genetic approach to test the hypothesis of PAP movement by the analysis of plant lines with SAL1 targeted to different subcellular compartments kindly provided by Kim and von Arnim (2009) and Rodríguez et al. (2010). In these earlier studies, the authors reported on partial complementation of morphological phenotypes, but neither PAP, nuclear gene expression, retrograde signaling, nor stress tolerance was measured in these studies.

First, does the chloroplast-localized SAL1 regulate PAP concentration? Given the unexpected dual targeting of SAL1 to the chloroplast and mitochondria, it was necessary to determine if chloroplast-localized SAL1 can modulate PAP levels. Targeting the yeast SAL1 (Sc-SAL1) to the chloroplast using the transit peptide of the Rubisco SSU resulted in a significant ( $P < 0.01$ ) lowering of PAP levels and *APX2* mRNA accumulation, demonstrating that chloroplast localization of SAL1 functions in regulating PAP content and *APX2* mRNA levels (Figures 5A and 5B).

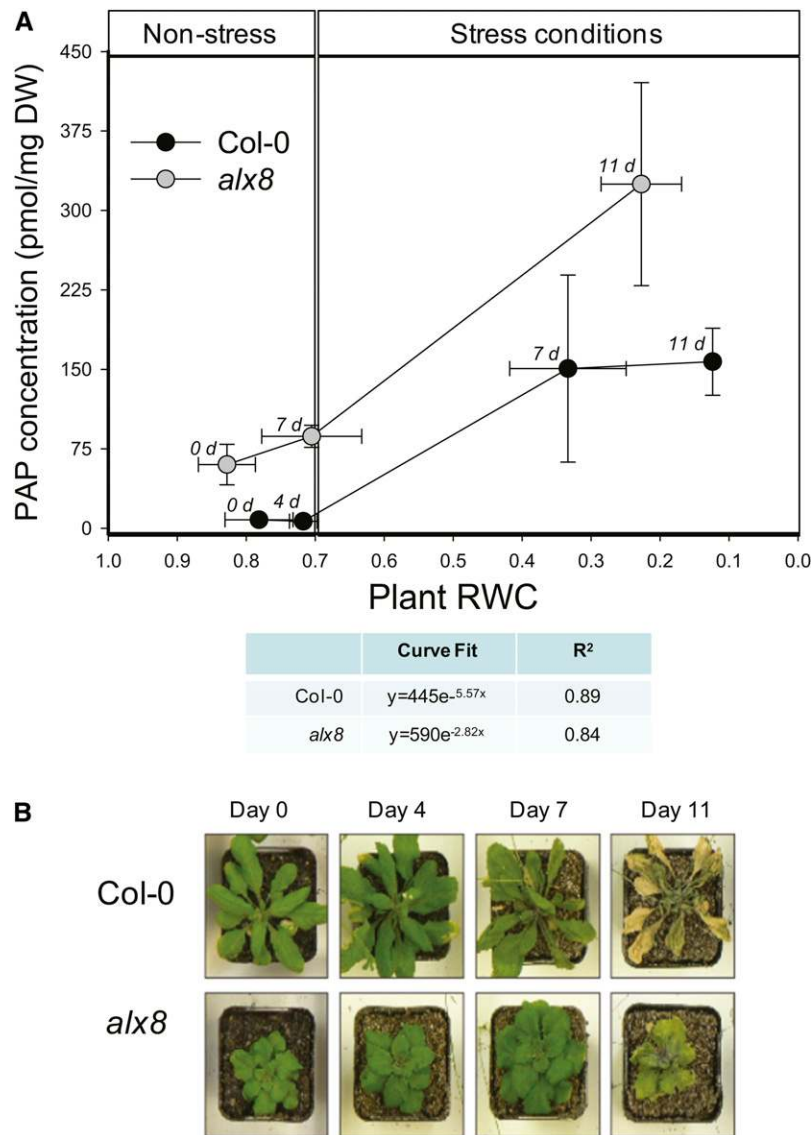


**Figure 3.** PAP Accumulates during Drought in *Arabidopsis*.

**(A)** Correlation between RWC of plants and PAP concentration on a dry weight (DW) basis  $\pm$  SD ( $n > 8$ ) during drought. The day in drought is indicated in italics. Measurements performed as in Figure 2 and Supplemental Figure 4 online. Data were fitted to exponential curves, and results are shown in the table ( $R^2$ , correlation coefficient). ANOVA two-factor analyses indicated a highly significant difference for day  $\times$  genotype for RWC and PAP ( $P < 0.005$ ). **(B)** Images of representative plants harvested for the PAP measurements performed in **(A)**.

Second, can PAP move between cellular compartments? Targeting of SAL1 to the nucleus resulted in complete complementation of PAP levels (Figure 5A), *APX2* mRNA abundance in LL and drought-stressed leaves, *ELIP2* mRNA abundance in LL- and HL-treated leaves, and the viability of plants in response to terminal drought (Table 2). The combined results of the targeting experiments indicate that the degree of complementation of PAP levels is somewhat proportional to the degree of complementation of *APX2* expression (Table 2, Figure 5). More importantly, they show that PAP can be catabolized by either nuclear or chloroplastic targeting of SAL1, demonstrating that PAP can move between subcellular compartments.

### SAL1 and Nuclear XRNs Coregulate a Large Subset of Genes

Given that PAP levels are elevated in *sal1* mutants, and PAP is known to inhibit the activity of the yeast XRNs (Dichtl et al., 1997; van Dijk et al., 2011), we hypothesized that PAP could regulate the expression of stress-responsive genes via attenuation of XRN-mediated RNA catabolism. Although the *Arabidopsis* XRNs are less well characterized than their *S. cerevisiae* counterparts, they play key roles in multiple RNA processing pathways and as post-transcriptional gene silencing suppressors (Kastenmayer and Green, 2000; Souret et al., 2004; Gy et al., 2007; Zakrzewska-Placzek et al., 2010). The XRNs belong to a small gene family in

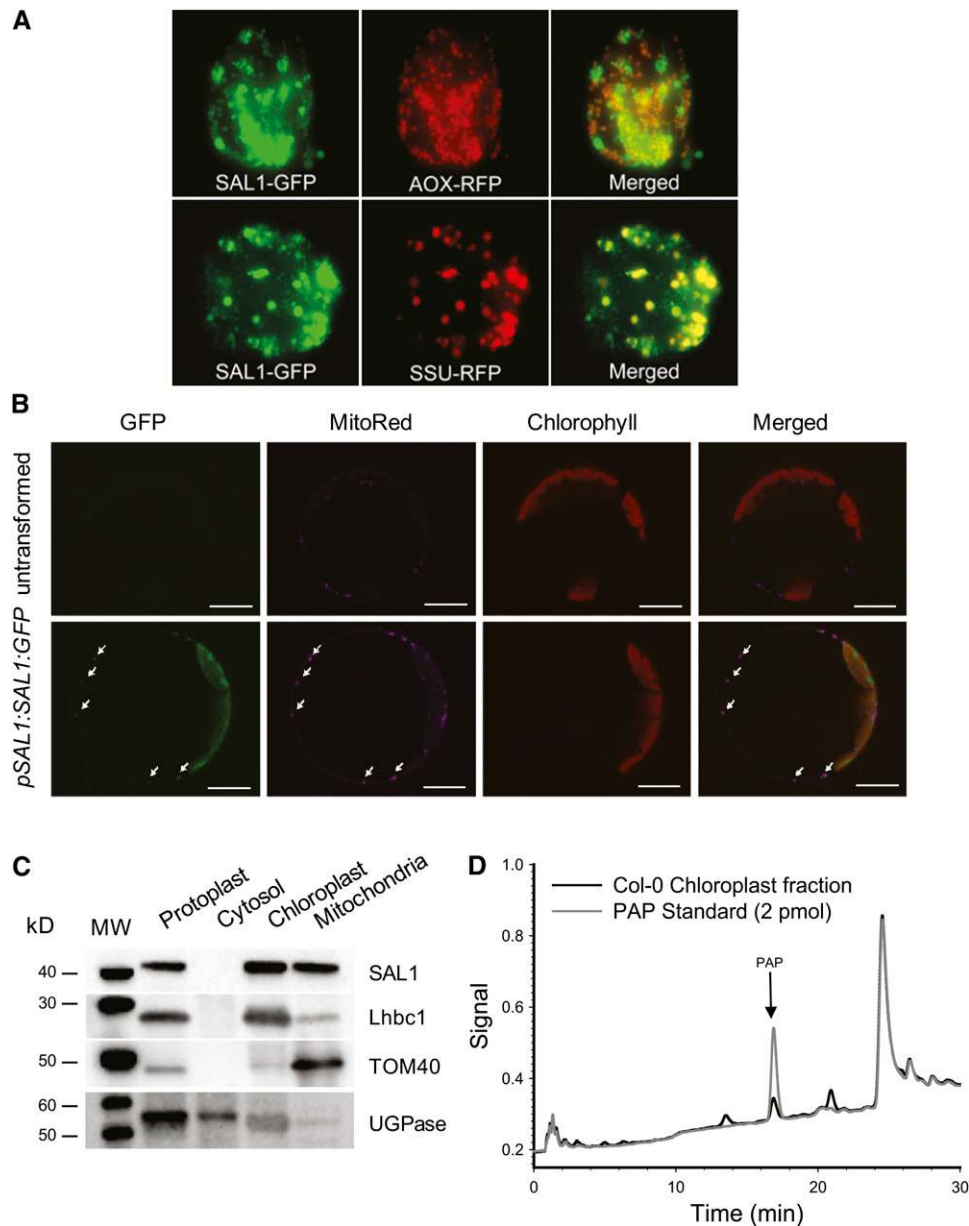


**Figure 4.** SAL1 Accumulates in the Chloroplasts and Mitochondria of *Arabidopsis*.

**(A)** Transient expression of *35S:SAL1:GFP* in *Arabidopsis* cells. The full-length cDNA encoding SAL1 was fused in frame with GFP and cotransformed into *Arabidopsis* cells with either mitochondrial-targeted RFP (AOX-RFP) or plastid-targeted RFP (SSU-RFP).

**(B)** Stable expression of the *SAL1:SAL1:GFP* fusion in *Arabidopsis* leaf mesophyll protoplasts. The endogenous *SAL1* promoter was fused to the *SAL1* genomic sequence (*pSAL1:SAL1:GFP*) and transformed into Col-0 plants. The same construct transformed into *sal1* mutants complemented all analyzed *sal1* phenotypes (Hirsch et al., 2011). The SAL1:GFP pattern was identical for several independent transgenic lines in the Col-0 background. White arrows indicate mitochondria. Bars = 12  $\mu$ m.

**(C)** Chloroplastic and cytosolic fractions were isolated from Col-0 protoplasts, while mitochondria were purified from seedlings using free-flow electrophoresis. Five micrograms of total protein was loaded per sample and subjected to immunoblots with polyclonal antibodies against SAL1 (Wilson et al., 2009) and other cellular markers.

**(D)** Detection of PAP in isolated Col-0 chloroplasts. Col-0 chloroplasts isolated using a Percoll gradient and assayed for PAP. The PAP peak for both the chloroplast extract and the PAP standard is indicated with an arrow.

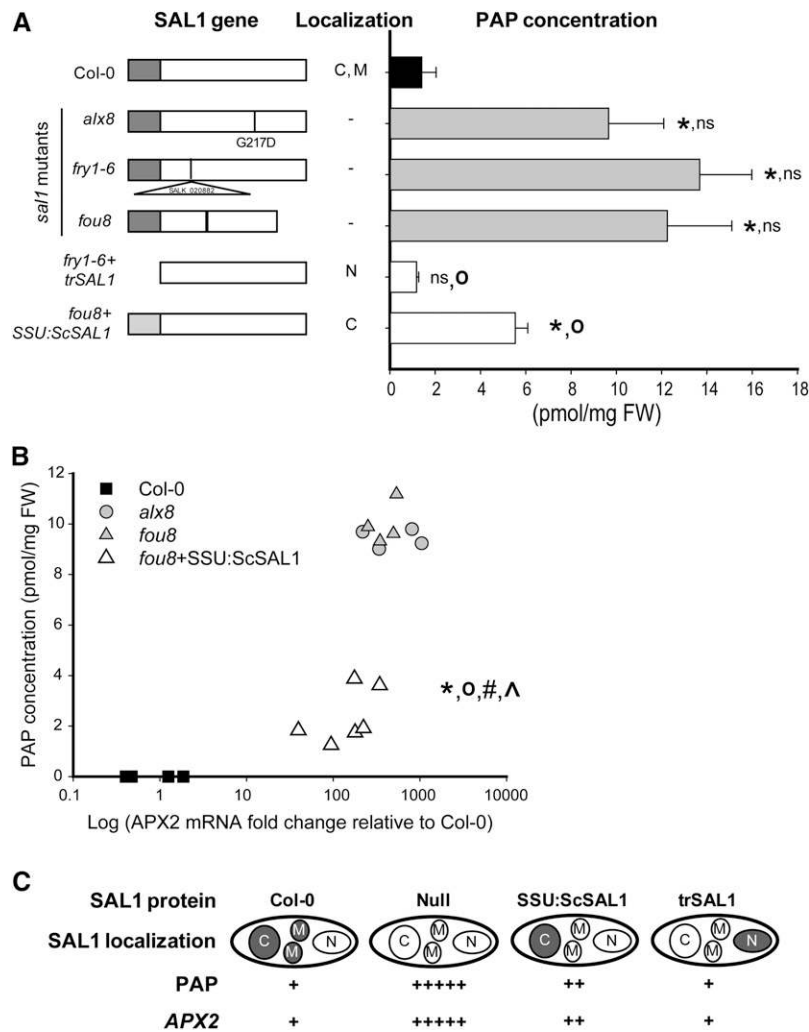


**Figure 5.** PAP Levels Can Be Lowered by Nuclear or Chloroplastic Targeting of SAL1.

**(A)** Schematic representations of the *SAL1* gene, mutant alleles, and constructs used to transform the corresponding genotypes. White boxes represent the mature protein, while the gray ones represent the transit peptides. The reported cellular location is indicated (C, chloroplast; M, mitochondria, N, nucleus; –, no *SAL1* protein). Bar graphs represent the average PAP concentrations from leaf tissue in pmol/mg FW  $\pm$  SD ( $n = 5$ ). Asterisk indicates significant difference relative to Col-0, and “<sup>ns</sup>” indicates significant difference to *alx8*. ns, not significant ( $t$  test;  $P < 0.01$ ).

**(B)** Correlation between PAP levels and *APX2* expression. The PAP concentration of 26-d-old plants was plotted versus the logarithm of the fold change of *APX2* mRNA relative to Col-0. Four biological replicates were run for Col-0, *alx8*, and *fou8* and six for *fou8*+*SSU:ScSAL1*. **(A)** and **(B)** show results from two different experiments. For PAP, asterisk indicates significant difference relative to Col-0, and “<sup>ns</sup>” indicates significant difference to *alx8* or *fou8*. ns, not significant ( $t$  test;  $P < 0.01$ ). For *APX2* mRNA, “<sup>#</sup>” indicates significant difference relative to Col-0, and “<sup>^</sup>” indicates significant difference to *alx8* or *fou8*. ns, not significant ( $t$  test;  $P < 0.01$ ).

**(C)** Schematic representation of the effect of *SAL1* cellular localization on PAP levels and *APX2* expression summarizing the results presented in Table 2 and **(A)** and **(B)**. Shaded compartments indicate the location of *SAL1* protein in each of the germplasm.

*Arabidopsis* with three members. XRN2 and XRN3 are homologs of Xrn2p/Rat1p and are nuclear localized. By contrast, the cytosolic XRN4 is a functional homolog of *S. cerevisiae* Xrn1p (Kastenmayer and Green, 2000). Identified substrates of XRN2 and XRN3 are excised hairpin loops that form part of precursor *MIRNA* transcripts, which also accumulate in *fry1-6* (Gy et al., 2007). On the other hand, XRN4 is involved in mRNA decay by degrading the resulting 3' cleavage products of microRNA (miRNA) targets (Souret et al., 2004).

Analysis of the *alx8* transcriptome revealed that transcripts for 19 genes that are confirmed targets of miRNAs were increased by at least threefold (see Supplemental Table 1 online). As probes for Affymetrix arrays are biased toward the 3' region of genes, we tested whether this reflected increased abundance of full-length mRNA or accumulation of cleaved transcripts due to inhibition of XRN4 by increased PAP levels. We undertook quantitative real-time PCR (qRT-PCR) of four miRNA targets using primers specific for 3' sequences or spanning the miRNA cleavage site (see



**Table 2.** Survival of and Expression Levels of Stress-Inducible Genes in Col-0, *alx8* Mutants, and *fry1-6* Complemented with SAL1 Directed to the Cytosolic-Nuclear Compartment

Genotype	Col-0	<i>fry1-6</i>	<i>fry1-6</i> + trSAL1	<i>alx8</i>
SAL1 protein <sup>a</sup>	Endogenous	–	Truncated	–
SAL1 location	C, M	–	N	–
Survival (days) <sup>b</sup>				
Experiment 1	7.7 ± 0.4 (7)	11.0 ± 0.4 (7)	8.1 ± 0.2 (14)	11.1 ± 0.3 (7)
Experiment 2	13.4 ± 0.2 (9)	17.0 ± 0.3 (6)	11.8 ± 0.2 (9)	15.2 ± 0.2 (8)
APX2 mRNA <sup>c</sup>				
Control	1 ± 0	661.7 ± 133.2	0.5 ± 0	313 ± 15.2
Drought	5.9 ± 1.3	501 ± 28.6	6.5 ± 1.9	274 ± 33.1
ELIP2 mRNA				
LL	1 ± 0.2	87 ± 63	1.5 ± 0.6	109 ± 19
HL	347 ± 93	3490 ± 993	711 ± 140	4191 ± 1336

<sup>a</sup>The SAL1 protein lacking the chloroplastic transit peptide (trSAL1) accumulates in the nucleus (N) (Kim and von Arnim, 2009). C, chloroplast; M, mitochondria; –, absent.

<sup>b</sup>Survival time, or the number of days plants remain viable, during drought was calculated as described by Woo et al. (2008) from measurements of the maximum efficiency of photosystem II ( $F_v/F_m$ ) using chlorophyll fluorescence. Values represent the average of days ± SE; numbers of replicates are indicated in parentheses. Two independent experiments were conducted at different times.

<sup>c</sup>The expression levels (fold change) of *APX2* in plants grown in control conditions or after 9 d of drought were measured by qRT-PCR. *ELIP2* message was quantified in the same manner but for plants after 1 h of LL or HL (1500  $\mu\text{mole m}^{-2} \text{s}^{-1}$ ). The values represent the relative mRNA levels compared to the Col-0 control ± SE ( $n = 3$ ).

Supplemental Figure 7 online). The uncleaved transcripts did not increase; rather, the 3' cleavage products for *ATHB15*, *PHB*, *MYB33*, and *REV* accumulated to higher levels in both *sal1* mutants compared with the wild type, with *MYB33* showing the highest increase (sixfold). The accumulation of 3' cleavage products in *alx8* that should otherwise be degraded by XRN3 is consistent with XRN3 being inhibited in SAL1 mutants.

To determine if XRN3 and SAL1-PAP regulate a common set of genes, we undertook gene expression profiling in the PAP-accumulating *alx8* mutant, *xm2 xm3* double mutant, and *xm4* (*ein5-6*, *ethylene-insensitive5*; Gregory et al., 2008). We used Affymetrix GeneChip *Arabidopsis* ATH1 genome arrays to analyze global changes in transcript abundance between Col-0 and the mutant genotypes. Whole rosettes of seedlings at the 10 true leaf stage of development were used for analysis of each genotype. We found that for *alx8* and *xm2 xm3*, there were 4038 and 2433 transcripts, respectively, that showed a significant change in transcript abundance (>1.5-fold, false discovery rate [FDR] corrected at  $P < 0.05$ ) relative to Col-0 (Figure 6A; see Supplemental Data Set 1 online). By contrast, only 156 transcripts were significantly altered in *xm4* compared with Col-0. This low level of transcriptome change in *xm4* is consistent with previous transcriptome profiling data of *xm4* (Souret et al., 2004; German et al., 2008; Gregory et al., 2008).

More importantly, there was a large and significant overlap between the *alx8* and *xm2 xm3* transcript profiles (Figure 6B). Of the 1404 genes upregulated in *xm2 xm3* (relative to Col-0), 50% (680 transcripts) were also upregulated in *alx8*, which is a significantly greater overlap than would be expected by random chance ( $P < 0.05$ ), while only 14 transcripts showed an antagonistic response (i.e., were downregulated in *alx8*), which is statistically fewer than would be expected by chance ( $P < 0.05$ ; see Supplemental Figure 8 online). Similarly, in the downregulated transcript set, there was a significant overlap of 64% (611 of 954 transcripts) between the *xm2 xm3* transcriptome and that of *alx8*, again with lower levels of antagonistic change than would be expected by random chance

(24 transcripts;  $P < 0.05$ ; see Supplemental Figure 8 online). Additionally, coexpression of four highly upregulated transcripts in the *alx8* microarray (Wilson et al., 2009) in *alx8* and *xm2 xm3* was confirmed by qRT-PCR (see Supplemental Table 2 online). Furthermore, the fold change of all genes upregulated by more than fivefold was also comparable for *xm2 xm3* and *alx8* (Table 3). Transcripts encoding transferases, transporters, hormone-related transcription factors, and starch synthase were coexpressed in both *alx8* and *xm2 xm3* to the same extent (Table 3).

Finally, comparison of all coexpressed genes up- or downregulated by more than threefold against a series of microarray experiments (Hruz et al., 2008) revealed a high degree of coexpression under HL, ABA, drought stress, and a combined moderate HL and mild drought on a plant with a defective mitochondrial stress-inducible protein, AOX1A (Giraud et al., 2008) (Figure 7). This same set of genes was not differentially expressed in LL or under different light quality and wavelengths, nor was the set similarly coexpressed upon treatment with the plastid translational inhibitor, lincomycin, that suppresses GUN-regulated genes. Both  $\text{H}_2\text{O}_2$ , known to induce some HL-responsive genes, and the mitochondrial respiratory complex I inhibitor, rotenone (Clifton et al., 2005; Garnier et al., 2008), resulted in increased expression of some of the upregulated genes, but the converse was observed for the downregulated genes. This suggests the coexpressed set of SAL1- and XRN3-regulated genes respond to specific organelle signals, such as HL, but not translational inhibitors, such as lincomycin.

### Nuclear XRN3 Regulate the Induction of HL and Drought Stress Genes

To investigate further the potential role of PAP in stress signal transduction pathways, we focused on the expression of the model chloroplast stress-responsive genes *ELIP2* and *APX2* in the *xm* mutants. Our analysis of *xm4/ein5-6* transcriptome data

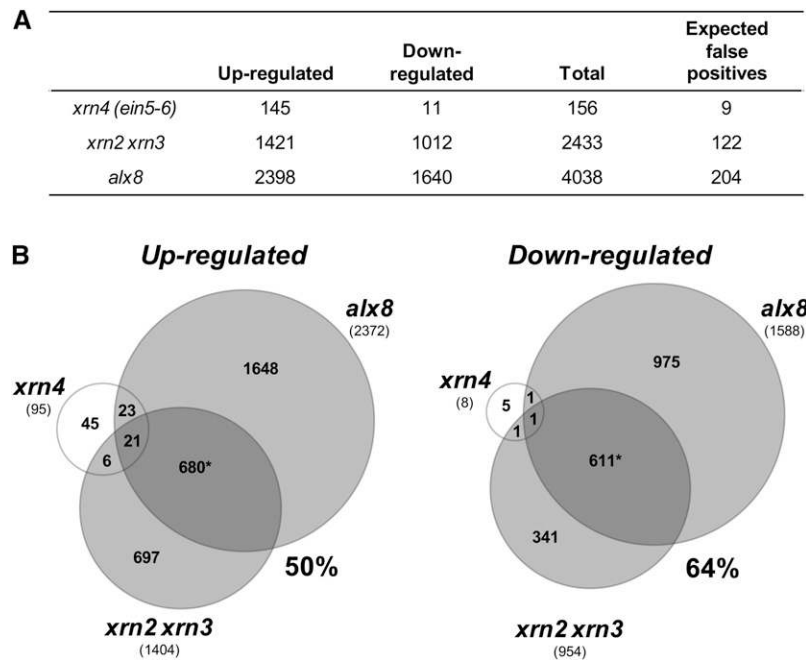


**Figure 6.** SAL1 and Nuclear XRN3 Regulate a Large Subset of Genes.

**(A)** Summary table of transcriptome changes in *xrn4*, *xrn2 xrn3*, and *alx8* mutants. Total number of genes whose transcripts were significantly different in abundance by >1.5-fold in each mutant compared with Col-0 after FDR correction at PPDE (>P) > 0.95 (95% confidence interval). Expected false positives at this FDR cutoff level are also indicated.

**(B)** Venn diagrams showing the overlap of changes in gene expression relative to Col-0 (>1.5-fold) between *alx8*, *xrn2 xrn3*, and *xrn4*. Numbers in the Venn diagrams indicate transcripts that are significantly (PPDE >P) > 0.95) up- or downregulated in the mutant genotype compared with Col-0. The percentage of genes in *xrn2 xrn3* that are regulated in the same manner as in *alx8* is given. The number of genes that significantly change excluding antagonistic changes is given in parentheses (see Supplemental Figure 8 online). Asterisk indicates significantly ( $P < 0.02$ ) more transcripts overlapping than expected by chance according to a  $\chi^2$  test.

(see Supplemental Data Set 1 online; Souret et al., 2004; German et al., 2008; Gregory et al., 2008) revealed that neither *ELIP2* nor *APX2* is upregulated in the *xrn4* mutant. Thus, we focused on XRN2 and XRN3.

We aimed to mimic PAP inhibition of the nuclear XRN3s by comparing the induction of stress-responsive genes between *xrn2 xrn3* and the *sal1* mutants under both LL and HL conditions. Indeed, mRNA levels of *ELIP2* were remarkably similar in *alx8*, *fr1-6*, and *xrn2 xrn3* mutants for nonstressed leaves, with *APX2* expression being induced in all three mutants but less so in *xrn2 xrn3* (Figure 8). Overall, all the mutants exhibited around 100-fold higher levels of *ELIP2* and 60- to 600-fold increased *APX2* compared with the wild type. Under HL stress, *ELIP2* was hyperinduced to the same extent (by ~3000-fold) in *alx8*, *fr1-6*, and *xrn2 xrn3*, and again this was not substantially different between the three mutants, yet it was 10-fold higher than the induction in Col-0 (Figure 8A). The results were comparable for *APX2*, with expression changes in *xrn2 xrn3* being of a similar order of magnitude to the *alx8* and *fr1-6* mutants, although attenuated (Figure 8B). This is consistent with the observations that *APX2* is regulated by multiple signaling pathways in response to HL stress, including  $H_2O_2$ , ABA, glutathione metabolism, and plastoquinone redox state (Karpinski et al., 1997; Fryer et al., 2003; Ball et al.,

2004; Rossel et al., 2006; Pogson et al., 2008; Galvez-Valdivieso et al., 2009) as well as PAP (Figure 5).

The results presented above clearly indicate that nuclear XRN3s are negative regulators of stress-inducible genes. Significantly, a triple mutant in both cytosolic and nuclear XRN3s was better able to survive drought when compared with the wild type in a soil-based experiment (Hirsch et al., 2011), indicating that XRN3s are regulators of the drought response. To elucidate whether cytosolic or nuclear XRN3s mediate the drought response, we investigated the degree of drought tolerance of nuclear *xrn2 xrn3* and *sal1* mutants, and we also included a second *xrn4* single mutant, *ein5-6* (Olmedo et al., 2006). Both *sal1* mutants survived the drought almost 50% longer compared with the wild type as previously shown (Wilson et al., 2009) (Figure 8C). Interestingly, plants with impaired nuclear XRN3 activity (i.e., the *xrn2 xrn3* mutant), but not those in which the cytosolic homolog was mutated (i.e., *xrn4*), survived longer than the wild type but not as long as the *sal1* mutants.

Taken together, these results suggest that PAP can stimulate gene expression by repressing the activity of the nuclear XRN3s. That is, XRN2 and XRN3 negatively regulate the expression of the stress-responsive genes *APX2* and *ELIP2* and the drought response, most likely via the SAL1-PAP signaling pathway.

**Table 3.** A Subset of Coreregulated Genes in *xrm2 xrm3* and *alx8* That Are Fivefold Up- or Downregulated Compared to Col-0

AGI <sup>a</sup>	Gene Description	<i>xrm2 xrm3</i> versus Col		<i>alx8</i> versus Col	
		F.C. <sup>b</sup>	P value	F.C.	P value
AT3G61630	CYTOKININ RESPONSE FACTOR6	109.3	1.48E-05	47.5	6.95E-07
AT2G04050	MATE efflux family protein	84.4	4.83E-07	19.5	6.95E-07
AT1G05680	UDP-glucuronosyl family protein	44.5	4.17E-08	7.4	6.95E-07
AT2G41730	Unknown protein	22.5	6.41E-10	10.4	6.95E-07
AT1G61800	Glc-6-phosphate transporter	19.4	4.92E-10	12.1	6.95E-07
AT2G04040	ATDXT1 transporter	18.1	3.07E-04	4.5	6.95E-07
AT2G21640	Unknown protein	16.7	1.13E-06	6.4	6.95E-07
AT3G53980	Lipid transfer protein family protein	16.0	4.58E-06	15.8	6.95E-07
AT5G08030	Glycerophosphoryl diester phosphodiesterase	15.0	3.00E-07	14.5	6.95E-07
AT2G40230	Transferase family protein	11.4	1.09E-09	11.8	6.95E-07
AT1G75580	Auxin-responsive protein, putative	9.2	6.14E-08	12.3	6.95E-07
AT5G25350	EIN3 BINDING F BOX PROTEIN2	7.5	2.42E-08	6.9	6.95E-07
AT5G27660	Ser-type peptidase/trypsin	6.9	1.67E-05	51.9	6.95E-07
AT1G56150	Auxin-responsive family protein	5.7	5.21E-09	6.5	6.95E-07
AT1G32900	Starch synthase, putative	5.1	9.05E-07	5.1	6.95E-07
AT2G22810	1-Aminocyclopropane-1-carboxylate synthase	-5.1	8.47E-05	-5.8	6.95E-07
AT4G25490	CBF1 transcription factor	-5.3	5.71E-06	-15.3	6.95E-07
AT5G26200	Mitochondrial substrate carrier family protein	-5.4	1.89E-07	-18.5	6.95E-07
AT5G18060	Auxin-responsive protein, putative	-5.5	5.30E-07	-8.9	6.95E-07
AT5G05250	Similar to unknown protein (TAIR: AT3G56360.1)	-6.2	1.87E-03	-15.5	6.95E-07
AT2G17880	DNAJ heat shock protein, putative	-6.5	3.31E-04	-15.4	6.95E-07
AT2G37950	Zinc finger (C3HC4-type RING finger) family	-8.6	2.96E-05	-17.9	6.95E-07
AT2G26710	BAS1 (PHYB SUPPRESSOR1)	-9.0	3.17E-07	-10.8	6.95E-07
AT2G44130	Kelch repeat-containing F-box family protein	-9.1	2.92E-07	-9.9	6.95E-07
AT5G54610	ANKYRIN; protein binding	-9.6	9.07E-05	-7.6	6.95E-07
AT1G78450	SOUL heme binding family protein	-14.9	3.98E-09	-12.5	6.95E-07

<sup>a</sup>AGI, Arabidopsis Genome Initiative.

<sup>b</sup>F.C., fold change compared to Col-0.

See Supplemental Data Set 1 online for the complete gene list.

## DISCUSSION

### PAP Is a Primary *In Vivo* Substrate of SAL1 and Accumulates in Response to HL and Drought Stress

Chloroplasts and mitochondria can be viewed as environmental sensors mediating cellular responses to external stimuli that result in short- and long-term acclimation responses, ranging from induction of stress-responsive genes to changes in leaf thickness and petiole length. Likewise, SAL1 has been linked to stress responses (Rossel et al., 2006; Wilson et al., 2009) and many developmental processes (Kim and von Arnim, 2009; Robles et al., 2010; Wilson et al., 2009; Rodríguez et al., 2010; Hirsch et al., 2011; Zhang et al., 2011), demonstrating that the enzyme influences multiple biological processes. This requires either multiple enzymatic activities or that the substrate of SAL1 can initiate multiple responses. Thus, understanding the enzymatic activity of SAL1 *in vivo* will shed light on many different fields of plant biology.

We addressed this issue by *in vivo* measurements of proposed substrates. The results presented here clearly support the view that PAP is a major *in vivo* substrate of the phosphatase SAL1 and not PAPS or IPs, as previously proposed (Xiong et al., 2001; Rodríguez et al., 2010; Zhang et al., 2011). First, a distinctive

peak corresponding to PAP was detected using HPLC coupled to fluorescence detection (Figures 2D; see Supplemental Figure 4 online). This method is more sensitive and specific than the absorbance detection used by Rodríguez et al. (2010), which could explain the lack of specific signal for PAP in that work, especially as PAP is very labile. Second, we were able to show that PAP increased by ~20-fold, whereas PAPS increased by just 1.6-fold (Table 1) and IPs either did not change (Figure 2) or increased by 1.5-fold to twofold (Zhang et al., 2011), which may be direct catalysis or an indirect effect, as many metabolites change in *sal1* mutants (Wilson et al., 2009). In this study, we measured sulfur metabolites (Cys,  $\gamma$ -EC, and GSH), adenosines (APS, PAPS, PAPS, SAM, Ade, AMP, ADP, and ATP), and inositols, none of which changed significantly or to the same degree as PAP. Thus, we consider that an indirect change in glutathione metabolism is not a consequence of the SAL1 mutation; thus, the increase in *APX2* mRNA in *alx8* is not a consequence of glutathione metabolism-mediated signaling as proposed for *rax1* (Ball et al., 2004). Furthermore, in a prior study, we measured the *alx8* metabolome using gas chromatography-mass spectrometry and of the metabolites that changed, such as carbohydrates and polyamines, and none could be readily viewed as likely substrates of a nucleotide phosphatase (Wilson

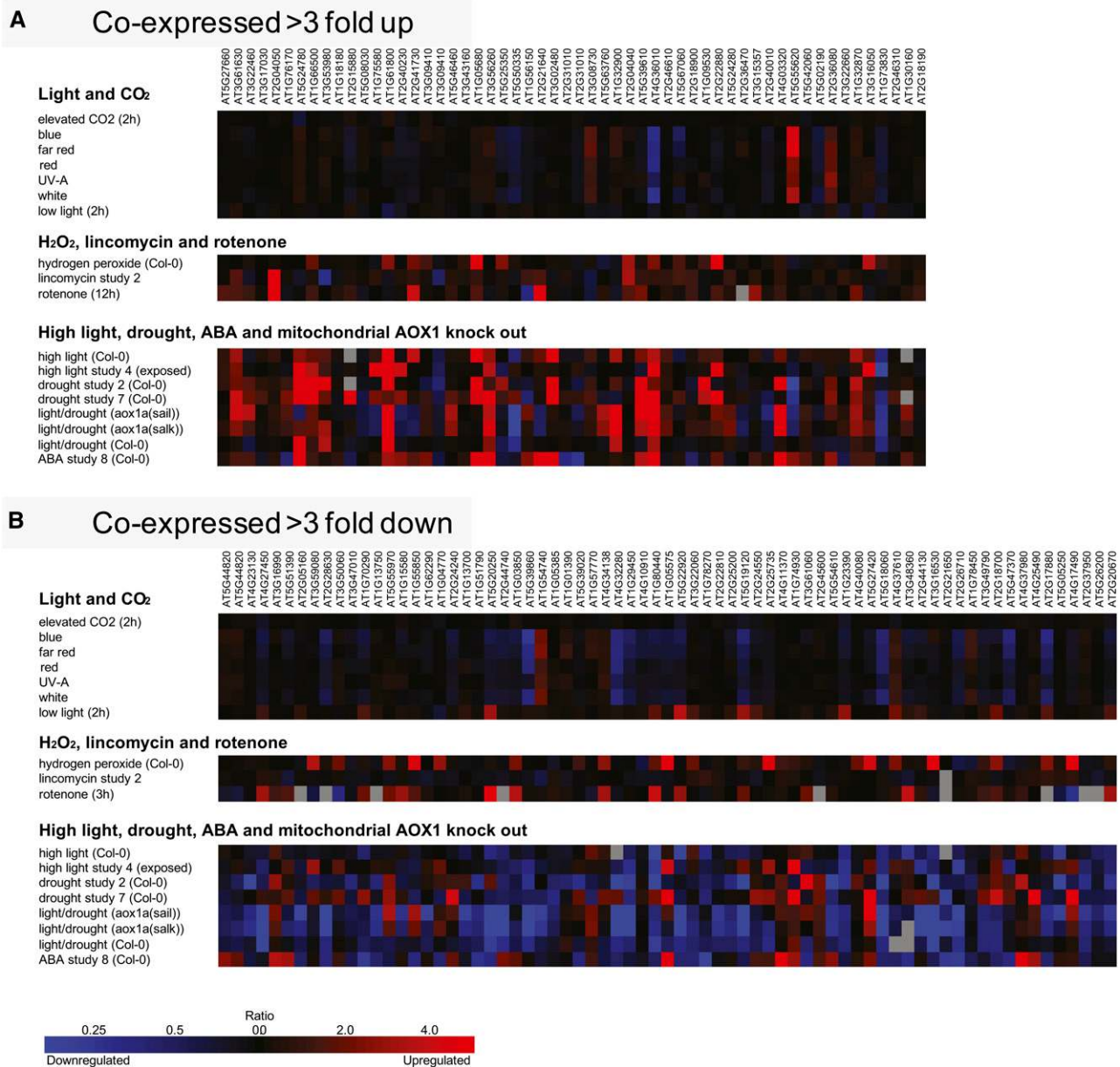


**Figure 7.** Heat Map of Genes Coregulated in both *alx8* and *xm2 xm3* Mutants.

Heat map of genes upregulated (**A**) and downregulated (**B**) threefold or more in both genotypes compared with their regulation in response to abiotic stress and chemical treatments (Hruz et al., 2008).

et al., 2009). Also, the expression of the PAP-specific phosphatase AHL enzyme that lacks IP<sub>3</sub> activity complements *sal1* mutants (Kim and von Arnim, 2009; Hirsch et al., 2011). This is also consistent with IP<sub>3</sub> not being important for drought tolerance in *Arabidopsis* (Perera et al., 2008). There is also a reported in vitro preference of the recombinant SAL1 enzyme for PAP (Gil-Mascarell et al., 1999; Xiong et al., 2001). Additionally, the *alx8* point mutation results in a recombinant SAL1 protein that cannot dephosphorylate PAP (Wilson et al., 2009). Thus, while we

cannot preclude another as yet unknown enzymatic activity for SAL1, we conclude PAP is a primary substrate of SAL1 in vivo.

If the basis of the altered response to HL and drought in *alx8* is mediated by increased PAP, then it might be expected that this metabolite should increase during stress in wild-type plants. Indeed, PAP increased 30-fold after 7 d of drought (Figure 3) and increased significantly within 1 h of HL stress. Interestingly, there was a tight correlation between leaf water status and PAP levels in both Col-0 and *alx8* plants.

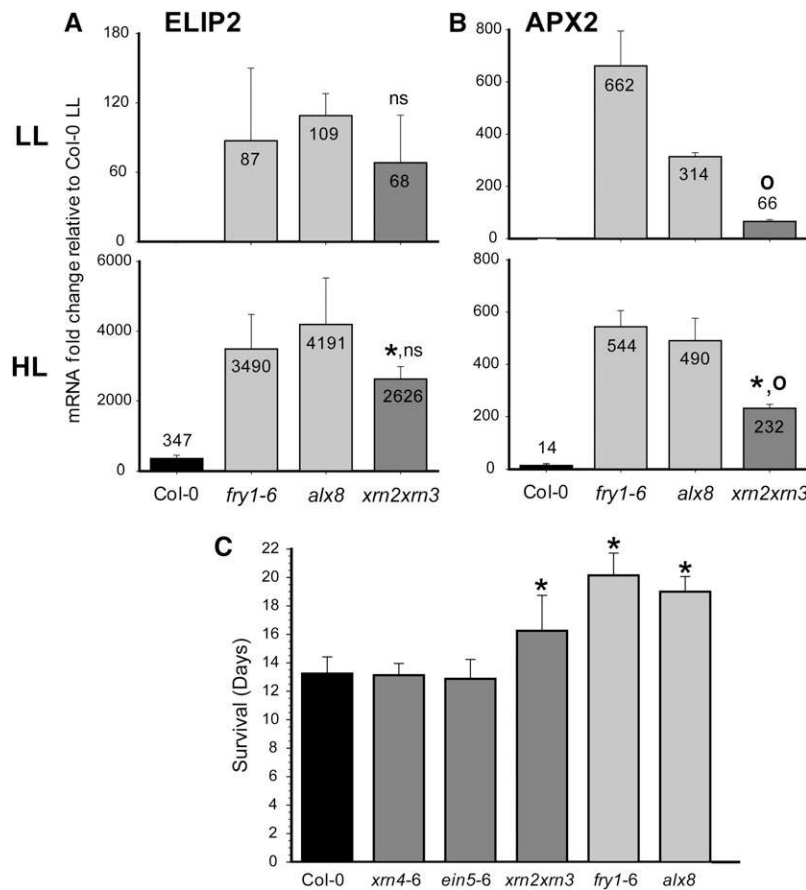


**Figure 8.** Light-Induced Gene Regulation and Drought Tolerance Is Similar in *sal1* and *xm2 xm3* Double Mutants.

**(A)** Expression levels of *ELIP2* after LL and HL.

**(B)** Expression levels of *APX2* after LL and HL.

For both **(A)** and **(B)**, the transcript levels were quantified by real-time PCR for both *alx8* and *xm2 xm3* mutants plants grown under standard growth conditions and after 1 h of HL stress ( $\sim 1500 \mu\text{mol m}^{-2} \text{s}^{-1}$ ). The bars represent the average of the fold change compared with that of the wild type  $\pm$  SD ( $n = 3$ ). For *xm2 xm3*, <sup>ns</sup> and ns indicate significant or no significant difference, respectively, relative to *sal1* mutants ( $t$  test;  $P < 0.05$ ). For HL, asterisk indicates significant difference relative to Col-0 HL ( $t$  test;  $P < 0.05$ ).

**(C)** Survival time of plants during drought calculated as described by Woo et al. (2008). Periodic measurements of the maximum efficiency of photosystem II ( $F_v/F_m$ ) using chlorophyll fluorescence were recorded during drought and used to calculate plant survival. Bar graphs represent the average survival time as measured in days  $\pm$  SD ( $n > 7$ ). Asterisk indicates significant difference relative to Col-0 ( $t$  test;  $P < 0.001$ ).

### SAL1 Localizes to Both Chloroplasts and Mitochondria

Critical to understanding the function of PAP is determining the subcellular localization of the enzyme that regulates its levels, SAL1. Conflicting reports have suggested that SAL1 fusions are targeted to nuclei (Kim and von Arnim, 2009), cytosol in the roots (Zhang et al., 2011), or chloroplasts of onion epidermal peels (Rodríguez et al., 2010). The reported nuclear localization of SAL1 (Kim and von Arnim, 2009) likely reflects the authors' use of a truncated SAL1 gene that lacked the transit peptide. To define the subcellular location of a protein, it is necessary to use multiple techniques, including *in vivo* analyses in the species of interest (Millar et al., 2009). Both stable and transient transformation lead to accumulation of SAL1:GFP in the chloroplast and mitochondria (Figures 4A and 4B), and the SAL1 protein was unequivocally

detected in the purified chloroplastic and mitochondrial fractions of Col-0 leaves (Figure 4C). Significantly, no SAL1 protein was detected in the cytosolic fraction, and effectively all SAL1:GFP fluorescence could be attributed to either chloroplasts or mitochondria, not nuclei (Figure 4).

The finding of SAL1 in the chloroplast is consistent with the chloroplastic localization of isoenzymes for the synthesis of APS and PAPS (Mugford et al., 2009) and the detection of SAL1 by chloroplast proteomic analysis (Peltier et al., 2006; Olinares et al., 2010). Thus, using three different approaches, we demonstrated that SAL1 is a dual-localized protein found in chloroplasts and mitochondria, not the cytosol or nucleus. In addition, SAL1 inactivation results in a 20-fold increase in PAP levels.

The detection of PAP in isolated chloroplasts demonstrates it can accumulate in this organelle. Interestingly, it is believed that

PAPS is largely synthesized in the plastid but that its conversion to PAP occurs in the cytosol. PAP could move back into the chloroplast via an unknown PAP/PAPS antiporter. This same proposed, but yet to be identified, transporter would allow its exit from the organelle back to the cytosol (Klein and Papenbrock, 2004; Mugford et al., 2009). An alternative to the PAP/PAPS antiporter is that movement is promoted by chloroplast damage during extreme stress. However, even photobleached cells contain viable and intact chloroplasts, as do *sal1* mutants (Wilson et al., 2009). Rather than membrane damage per se enabling movement, it is more likely that stress can modulate the transport of proteins or signaling molecules, such as PAP. Regardless of the mechanism of transport, the lowering of PAP to near-wild-type levels by targeting Sc-SAL1 to the chloroplast demonstrated that PAP can move from the site of synthesis in the cytosol to the chloroplast.

The observation that SAL1 was also found in mitochondria was unexpected and raises the question as to its role and enzymatic activity in that organelle. Whereas it is beyond the scope of this study, it is worth noting that the partial complementation observed in *sal1* mutants by Sc-SAL1 targeted to the chloroplast could reflect a reduced expression or activity of the yeast enzyme in transgenic *Arabidopsis* or a mitochondrial role for SAL1. Additionally, knockouts of a nuclear gene, *AOX1A*, encoding a mitochondrial protein used to study mitochondrial retrograde signaling (Giraud et al., 2008) resulted in similar coexpression of genes in response to a moderate drought and light as those coexpressed in *alk8* and *xm2 xm3*, and a possible, but weaker, correlation was observed for the mitochondrial electron transporter chain inhibitor, rotenone (Figure 7).

### Evidence for a SAL-PAP Retrograde Pathway

Two studies have reported on the complementation of the morphological phenotypes of *sal1* mutants by targeting SAL1

to the nucleus (Kim and von Arnim, 2009) and Sc-SAL1 to the chloroplast (Rodríguez et al., 2010). However, the significance of these findings with respect to PAP acting as a retrograde signal was not considered by the authors; rather, they concluded that their constructs demonstrated the location of SAL1. PAP levels, chloroplast-specific responses, and drought responses were not measured. Furthermore, as mentioned above, the differing reported localizations of SAL1 have prevented any systematic analysis.

In this study, we demonstrated that total leaf PAP pools can be significantly lowered by targeting Sc-SAL1 exclusively to the chloroplast (Figure 5) and that induction of the nuclear gene *APX2*, which is routinely used to study HL and drought stress-induced retrograde signaling, was lowered when PAP was lowered by chloroplastic SAL1 complementation.

There are several lines of evidence that support the notion that PAP can move between cellular compartments, as shown in Figure 9. First and most compelling is that nuclear targeting of SAL1 results in the full complementation of *sal1* mutant phenotypes, including total leaf PAP levels, *APX2* expression in LL and drought, *ELIP2* expression in LL and HL, and drought tolerance (Figure 5, Table 2). Second, *sal1* and *xm2 xm3* double mutants show a very similar molecular and morphological phenotype, suggesting that PAP accumulation can inhibit XRN function as originally proved in yeast (Dichtl et al., 1997) and suggested to occur in plants (Gy et al., 2007). Indeed, it is reasonable to assume that once in the cytosol, PAP would diffuse freely through the nuclear pore as do other nucleotides. Thus, degradation of PAP pools in either the chloroplast, mitochondria, or nucleus have the potential to restore the wild-type phenotype at the molecular level. This could be interpreted as PAP being able to move between cellular compartments.

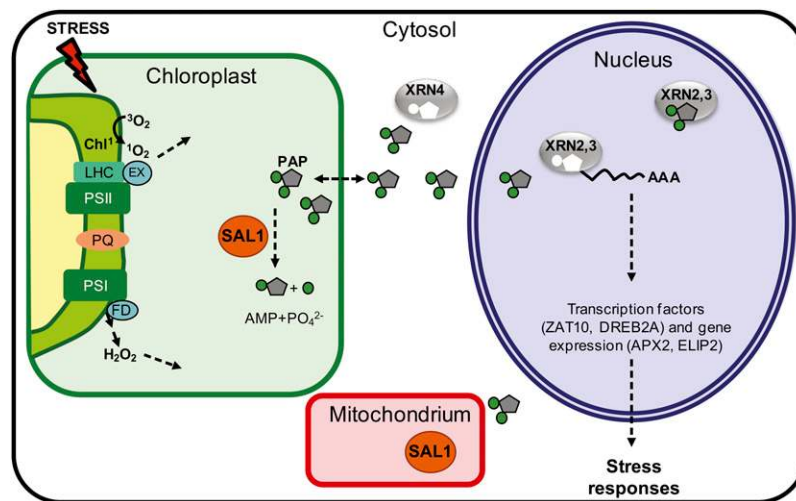


**Figure 9.** Proposed Model for a SAL1-PAP Retrograde Signaling Pathway.

PAP levels are negatively regulated by the chloroplastic SAL1 phosphatase (Figures 2 to 5). Upon environmental stresses, such as HL and drought, PAP levels increase (Figure 3). PAP can move between cellular compartments as evidenced by the complementation studies (Figure 5). Elevated PAP levels likely inhibit XRNs in the cytosol and nucleus. Nuclear XRN inhibition causes similar changes in expression to *sal1* mutants, such as *ELIP2* and *APX2*, and a degree of drought tolerance (Figures 6 to 8, Table 3).

[See online article for color version of this figure.]

Given the effectiveness of nuclear complementation, it begs the question as to why SAL1 is targeted to the organelles and not the nucleus. One speculative option is that this provides the potential to regulate PAP content in the cell in response to environmental stimuli. How, for instance, are HL and drought regulating PAP accumulation and/or transport? The observed increase in PAP levels during drought in *alx8* plants lacking SAL1 suggests that PAP pools may be regulated at least in part by increased biosynthesis of PAP rather than a decrease in catabolism. However, whether SAL1 activity is directly regulated by HL and drought is not known, nor is it known if the stress-mediated PAP accumulation precedes ABA accumulation or not. Additionally, it would be worth investigating whether there could be regulation of PAP movement between compartments. Given the relatively small but significant change in PAP in response to HL, it might be that relocation of PAP within the cell also contributes to the response.

Does the proposed retrograde pathway operate in parallel or series with other proposed retrograde pathways? The gene expression profiles of other retrograde mutants pertain to the specific signals being studied, such as the repression of *Lhcb* mRNA in response to lincomycin and the chloroplast bleaching herbicide, NFZ, in the GUN signaling cascade. *Lhcb* mRNA does not change in *alx8*, and few of the coexpressed *alx8* and *xm* genes are induced or repressed by lincomycin (Figure 7; see Supplemental Data Set 1 online). Given the low levels of hydrogen peroxide in *sal1* mutants (Figure 1), it is unlikely that the SAL1-PAP pathway is epistatic to or regulated by H<sub>2</sub>O<sub>2</sub>. With respect to ABA, the increase in PAP during drought and the induction of drought and ABA-responsive genes in *sal1* and *xm* mutants would suggest some interaction (Figures 3 and 7). Both drought and light alter chloroplasts and initiate gene expression changes, as demonstrated by the initial isolation of the *alx8* mutant that results in changed expression of chloroplast proteins (ELIP2) and cytosolic proteins (APX2) and confers cellular tolerance to stress (e.g., plasma membrane damage) (see Wilson et al., 2009) and lowers ROS (Figure 1). That is, while drought is a general stress on a cell, a component of the drought response can be viewed as chloroplast specific, namely, inhibition of photosynthesis, leading to elevated ROS. Thus, it is not unexpected that 70% of HL genes are drought inducible. However, that does not preclude other drought response pathways operating independently or concurrently with the proposed SAL1-PAP pathway.

### Evidence for XRN5s Being Targets of the SAL1-PAP Pathway

A key question is, what are the targets of PAP? PAP is an adenosine phosphate and thus can bind irreversibly to yeast XRN5s, inhibiting their activity (Dichtl et al., 1997). Thus, we investigated whether *xm* knockouts would phenocopy elevated PAP levels.

Whereas the single *xm* mutants show a wild-type phenotype, there is a strikingly similar expression levels of 56% of transcripts altered in *xm2 xm3* with those in *alx8*, similar drought tolerance of the *xm2 xm3* (Figures 6 to 8, Tables 2 and 3), and similar altered leaf morphology (Gy et al., 2007). All of this suggests that XRN2 and XRN3 are negative regulators of stress gene expression and may function in the SAL1-PAP pathway. *xm4* is also likely to be inhibited by elevated PAP; here, we show *alx8* alters the abundance of the 3' cleavage products of four miRNA targets (see

Supplemental Figure 7 online), in addition to those reported for *xm4-5* (Souret et al., 2004) and the *sal1* mutants *fry1-4* and *fry1-5* (Gy et al., 2007). Based on gene expression analysis (Figures 6 and 7) and *xm4* phenotypes, it is unlikely that inhibition of XRN4 accounts for the majority of the phenotypes observed in *alx8*, as the majority of the transcript changes, altered morphology, and drought tolerance better correlate with the *xm2 xm3* double mutant. With respect to the drought tolerance, UDP-glucuronosyl/UDP-glucosyl transferase family protein (AT1G05680) is significantly upregulated in both *sal1* and *xm2 xm3* mutants (see Supplemental Data Set 1 online), and increasing its levels can cause drought tolerance (Tognetti et al., 2010). However, *xm2 xm3* plants are not as tolerant as *alx8* plants, and ~40% of the *alx8* transcriptome changes are not found in the *xm2 xm3* arrays. Although it remains to be directly demonstrated that PAP inhibits the activity of plant XRN5s, the weight of evidence presented here and by Gy et al. (2007) is in favor of this interaction. Whether there are other targets for PAP or processes altered by SAL1 is the subject of investigation.

XRN-mediated gene regulation does not consist just of altered mRNA degradation as for *MYB33* (see Supplemental Figure 7 online) but also includes elevated transcription, as demonstrated by *APX2:LUC* (Rossel et al., 2006). We envisage at least two potential mechanisms of action: XRN5s alter mRNA levels by altering small and/or cleaved RNA pools, or XRN5s alter gene transcription by affecting transcription termination. With respect to the latter, XRN5s alter the release of RNA polymerases from the gene, thereby affecting transcription in yeast and human (Kim et al., 2004; West et al., 2004). Regarding changes to gene silencing, XRN5s may inhibit accumulation of small RNAs that target positive regulators of stress gene expression. Alternatively, inhibition of the XRN5s by PAP could prevent the degradation of the uncapped RNA templates triggering post-transcriptional gene silencing (Gy et al., 2007) of genes that repress stress responses. The determination of the substrates and the function of the nuclear XRN5s will be critical to elucidate the underlying gene regulatory mechanisms.

In this article, we provide evidence for a previously undiscovered retrograde mechanism, the SAL1-PAP pathway, which would rely on chloroplastic SAL1 enzyme-regulating PAP levels, thereby affecting its action on nuclear targets, most likely XRN5s. We resolve the chloroplastic localization of SAL1 and provide the unreported finding that it also accumulates in mitochondria but not in the cytosol or nuclei and that a primary *in vivo* substrate is PAP. PAP accumulates as result of HL and drought (20-fold), and it correlates with upregulation of 25% of the HL transcriptome. PAP is known to inhibit yeast XRN5s, and we show here that SAL1 and XRN5s mediate accumulation of 3' mRNA cleavage products and expression of a common set of genes. Based on this, together with our finding that PAP can be depleted by targeting SAL1 to chloroplasts or nuclei, we conclude that SAL1 and PAP function in one of the cellular retrograde signaling pathways.

## METHODS

### Plant Material and Growth of Plants

Plant growth and drought stress conditions were as previously described (Wilson et al., 2009). Seeds from *fry1-6* (SALK\_020882) overexpressing a

truncated form of *SAL1* (AT5G63980) cDNA (Kim and von Arnim, 2009) and the *xrm2-1 xrm3-1* (*xrm2 xrm3*) double mutant (Gy et al., 2007) were donated by A.G. von Arnim (University of Tennessee). Seeds for *fou8* and SSU:ScSAL1-complemented *fou8* (Rodríguez et al., 2010) were kindly provided by E.E. Farmer (University of Lausanne). Survival time of plants during drought was calculated as described by Woo et al. (2008) from measurements of the maximum efficiency of photosystem II ( $F_v/F_m$ ) using chlorophyll fluorescence. *xrm4* mutants were *xrm4-6* (SALK\_014209) and *ein5-6* (Olmedo et al., 2006). All insertion mutants were confirmed by PCR. See the primers listed in Supplemental Table 3 online.

### RNA Isolation and RT-PCR

Total RNA was extracted from ~50 mg of leaf tissue using the Spectrum Total RNA kit (Sigma-Aldrich). RNA was reversed transcribed into cDNA using the Roche Transcriptor first-strand cDNA synthesis kit (Roche Diagnostics) and oligo(dT) primers. Gene expression was analyzed on a Roche LightCycler480 using hydrolysis probes from the Universal Probe Library and applying the relative quantification method described by Pfaffl (2001). Samples were normalized against *CYCLOPHILIN5* (AT-CYP5, AT2G29960) or *GLYCERALDEHYDE-3-PHOSPHATE DEHYDROGENASE C2* (*GAPC2*, AT1G13440). At least three biological replicates per genotype per experiment were sampled, and each sample was run in triplicate.

### Global Transcript Analyses

Analysis of the changes in transcript abundance between Col-0, *xrm4* (*ein5*), *alx8*, and *xrm2 xrm3* seedlings was performed using Affymetrix GeneChip *Arabidopsis* ATH1 genome arrays. Whole rosettes from several seedlings at the 10 true leaf stage of development (synchronized for development to account for the slower growth rate of *alx8*), grown under a 16-h photoperiod, were pooled for each biological replicate. Col-0 and mutant tissue samples were collected in biological triplicate. For each replicate, total RNA was isolated from the leaves using the RNeasy plant mini protocol (Qiagen) and quality verified using a Bioanalyzer (Agilent Technologies), and spectrophotometric analysis was performed to determine the  $A_{260}:A_{280}$  and  $A_{260}:A_{230}$  ratios. Preparation of labeled copy RNA from 400 ng of total RNA (3' IVT Express kit; Affymetrix), target hybridization, as well as washing, staining, and scanning of the arrays were performed exactly as described in the Affymetrix GeneChip expression analysis technical manual, using an Affymetrix GeneChip Hybridization Oven 640, an Affymetrix Fluidics Station 450, and an GeneChip Scanner 3000 7G at the appropriate steps.

### Statistical Analysis

Data quality was assessed using GCOS 1.4 before CEL files were exported into AVADIS Prophetic (version 4.3; Strand Genomics) and Partek Genomics Suite software, version 6.3, for further analysis. MAS5 normalization algorithms were performed only to generate present/absent calls across the arrays. Probe sets that recorded absent calls over 11 or more of the gene chips analyzed were removed. Bacterial controls were also removed, resulting in a final data set of 16,022 probe identifiers. CEL files were also subjected to GC-content background Robust Multi-array Average normalization for computing fluorescence intensity values used in further analyses. Correlation plots were examined between all arrays using the scatterplot function in the Partek Genomics Suite, and in all cases  $r \geq 0.98$  (data not shown). The values of gene expression after normalization with GC-content background Robust Multi-array Average were analyzed to identify differentially expressed genes by a regularized  $t$  test based on a Bayesian statistical framework using the software program Cyber-T (Baldi and Long, 2001) (<http://cybert.microarray.ics.uci.edu/>). Cyber-T employs a mixture

model-based method described by Allison et al. (2006) for the computation of the global false-positive and false-negative levels inherent in a DNA microarray experiment. To accurately control for FDR and minimize false positives within the differential expression analysis, posterior probability of differential expression PPDE(P) values and PPDE(>P) values were calculated, as a means to measure the true discovery rate ( $1 - \text{FDR}$ ). Changes in transcript abundance were considered significant with a PPDE(>P) > 0.95 and a fold change > 1.5-fold.

Overlaps in the transcript abundance responses for the different genotypes were plotted on Venn diagrams to determine statistically significant over- or underrepresentation in the overlap, compared with that which is expected by random chance, using a Pearson's  $\chi^2$  test for independence.

ANOVA and  $t$  test analyses were performed using Microsoft Excel.

### Cell Fractionation

*Arabidopsis thaliana* ecotype Col-0 was grown in 0.5× Murashige and Skoog (MS) medium, 1% (w/v) Suc, and 0.7% (w/v) agar plates under LL (100  $\mu\text{mol photon m}^{-2} \text{ s}^{-1}$ ) with a 12-h photoperiod at  $20 \pm 2^\circ\text{C}$  for 16 d. Approximately 13 g of seedlings were harvested in the morning before commencement of the light period. The tissue was vacuum infiltrated in 40 mL of digestion medium (1.5% [w/v] cellulase, 0.4% [w/v] macer-ozyme, 0.5 M Suc, 20 mM KCl, 10 mM  $\text{CaCl}_2$ , and 20 mM MES) for 30 min and incubated for an additional 3 h. All incubation steps were performed in the dark. After incubation, the mixture was filtered through two layers of miracloth presoaked in floating medium (Gardeström and Wigge, 1988) (0.5 M Suc, 1 mM  $\text{MgCl}_2$ , and 5 mM HEPES, pH 7.0). Protoplasts were released by passing the eluant through the slurry several times, pressing it with a spatula after the last elution, and collecting it in a glass beaker in ice. All subsequent steps were performed at  $4^\circ\text{C}$ . The dark-green flow-through was divided into 10-mL aliquots in four 30-mL Corex tubes and topped with 5 mL of floating medium II (FMII; 0.4 M Suc, 0.1 M sorbitol, 1 mM  $\text{MgCl}_2$ , and 5 mM HEPES, pH 7.0) and 3 mL of floating medium III (FMIII; 0.5 M sorbitol, 1 mM  $\text{MgCl}_2$ , and 5 mM HEPES, pH 7.0). This was performed very carefully to avoid disrupting the interfaces between the different solutions. The tubes were centrifuged at 250g for 5 min at  $4^\circ\text{C}$  in a swing-out rotor (brake off). Intact protoplasts were recovered from the FMIII/FMII interface and the chloroplast-containing pellet further processed (see below). The intact protoplasts were disrupted by six strokes in a prechilled 10-mL Wheaton Potter-Elvehjem tissue grinder. An ~8-mL sample was transferred to a 15-mL Corex tube, a 500  $\mu\text{L}$  85% (v/v) Percoll cushion was layered at the bottom with a long glass Pasteur pipette, and a 1000- $\mu\text{L}$  layer of FMIII was added on the top. The gradient was then centrifuged at 2000g for 10 min at  $4^\circ\text{C}$  in a swing-out rotor (brake off). Contaminating protoplasts settled in the FMIII/sample interface, and the remainder of the chloroplasts were on top of the 85% (v/v) Percoll cushion. The middle phase, containing the cytosolic fraction, was carefully removed and centrifuged at 13,000g for 30 min at  $4^\circ\text{C}$  in a fixed-angle rotor to remove any contaminating organelles. The supernatant was further concentrated with 5-kD Ultrafree centrifugal filter devices (Millipore).

For the purification of chloroplasts, the pellets after the first centrifugation step were resuspended in a final volume of 10 mL of chloroplast buffer (50 mM HEPES-KOH, pH 8.0, 5 mM EDTA, 5 mM EGTA, 330 mM sorbitol, 5 mM Cys, and 5 mM ascorbic acid) and cleared by centrifugation at 250g for 5 min at  $4^\circ\text{C}$  in a swing-out rotor. The pellets were gently resuspended in a minimum volume (~3 mL) of the same buffer, loaded onto a 45/85% (v/v) Percoll gradient (Aronsson and Jarvis, 2002), and spun at 3000g 15 min at  $4^\circ\text{C}$  in a swing-out rotor (brake off). The intact chloroplasts were recovered from the 45/85% (v/v) interface, washed once with 10 volumes of chloroplast buffer, and spun at 800g for 15 min in a swing-out rotor at  $4^\circ\text{C}$ . The clean, intact chloroplasts were resuspended in 500  $\mu\text{L}$  of chloroplast buffer.



Mitochondria were purified by free-flow electrophoresis as described by Eubel et al. (2007).

### Protein Gel Electrophoresis and Immunoblotting

Total protein from tissue and cell fractions were extracted in 10% (w/v) tricarboxylic acid in cold acetone. Protein gel electrophoresis was performed as described (Wilson et al., 2009). Immunoblotting was performed using the SNAPid system (Millipore) and antibodies against SAL1 (1:1000; Wilson et al., 2009), Lhcb2 (1:1000; Agrisera AS01-003), TOM40 (1:5000; Carrie et al., 2009), and UGPase (1:500; Agrisera AS05-086).

### GFP Fusion for Subcellular Localization

The full-length cDNA of *SAL1* was cloned as a C-terminal GFP fusion by Gateway cloning under the control of a 35S promoter (Murcha et al., 2007; Carrie et al., 2009). Primers used were as follows: SAL1FOR, 5'-GGG-GACAAGTTTGTACAAAAAGCAGGCTTGAAGGAGATAGAACCATG-ATGCTATAAATGTTTTCCGAA-3', and SAL1REV, 5'-GGGGACCAC-TTGTACAAGAAAGCTGGGTCTCCACCTCCGGATCCGAGAGCTGAA-GCTTCTCTTGC-3', where underlined sections correspond to SAL1 and the rest for homologous recombination. The PCR product was cloned into pDonr201 (Invitrogen) and then into pDest/pGem/CGFP (Carrie et al., 2009). The plastid localization control, Rubisco SSU, and the mitochondrial control, AOX1, were cloned as C-terminal RFP fusions using the same system. SAL1-GFP along with either one of the control constructs was cotransformed into *Arabidopsis* cell suspension as previously described (Thirkettle-Watts et al., 2003; Carrie et al., 2009). Localization of GFP and RFP expression was conducted using an Olympus BX61 fluorescence microscope and imaged using the CellIR imaging software as previously described (Carrie et al., 2007; Murcha et al., 2007).

### In Vivo SAL1:GFP Visualization

The SAL1 genomic fragment (1960 bp) and an additional 753-bp upstream region was PCR cloned by standard molecular techniques in the Wassilewskija accession. Primers used were as follows: FRY1promF, 5'-CACCGTTGGAGATTATCTTCTGTAGG-3', and FRY1endR, 5'-GAG-AGCTGAAGCTTTCTCTTGC-3', which amplified a product of 2713 bp (753+1960). After sequencing in pENTR/D-TOPO, an LR clonase reaction was used to clone the genomic fragment in the binary vector pGWB4 (Nakagawa et al., 2007) and transformed into *Arabidopsis* Col-0 by simplified floral dip method (Logemann et al., 2006). Primary transformants were selected in medium containing 50  $\mu$ g/L hygromycin. Their progeny were screened for GFP expression in standard in vitro growth conditions.

Observations were made using either an upright DMR or a Leica SP2 AOBS inverted confocal microscope (Leica Microsystems). In the first case, a  $\times 10$  DRY objective lens (numerical aperture of 0.40) was mounted on an upright DMR microscope equipped with a mercury lamp. The GFP and chlorophyll signals were collected using a 515-nm-long pass filter (excitation with 450 to 490 nm). For the observations made with the Leica SP2 AOBS inverted confocal microscope, 2-week-old plants grown in soil in short-day conditions were used. A  $\times 10$  dry objective lens (numerical aperture of 0.40) was used for all observations. GFP and chlorophyll were excited with a 488-nm argon laser. The GFP signal was collected at 496 to 539 nm and chlorophyll at 676 to 718 nm (pinhole adjusted to 2.46). Following acquisition, brightness and contrast were adjusted using the LCS software.

Mesophyll protoplasts were prepared as described (Leonhardt et al., 2004). Protoplasts were incubated on ice with 400 nM MitoTracker Red CMXRos (Invitrogen) for 30 min, in the dark, before confocal observations. Observations were made using a Leica SP2 AOBS inverted confocal microscope (Leica Microsystems) equipped with an argon ion laser

and a DPSS 561-nm laser. A  $\times 63$  water objective lens (numerical aperture of 1, 20) was used for all observations. GFP was excited at 488 nm and MitoTracker red at 561 nm. The GFP signal was collected at 500 to 530 nm, the MitoTracker Red signal was collected at 575 to 615 nm, and chlorophyll at 653 to 731 nm. Following acquisition, brightness and contrast were adjusted using the LCS software (identical parameters were applied to control and GFP images).

### Quantification of Phosphoadenosines

#### Extraction of Adenosine Derivatives

Adenosine derivatives were extracted in HCl and quantified fluorometrically after specific derivatization of adenosine compounds with chloroacetaldehyde (CAA) based on a method previously described (Bürstenbinder et al., 2007). Briefly, 100 mg of tissue was ground in liquid nitrogen, extracted with 1 mL of 0.1 M HCl in ice for 15 min, and centrifuged twice at 16,000g at 4°C for 5 min. After clarification, 150  $\mu$ L of the supernatant mixed with 770  $\mu$ L of CP buffer [620 mM citric acid-1-hydrate and 760 mM (Na)<sub>2</sub>HPO<sub>4</sub>·2H<sub>2</sub>O, pH 4] was derivatized by adding 80  $\mu$ L of 45% (v/v) chloroacetaldehyde for 10 min at 80°C. The sample was finally centrifuged at 16,000g for 45 min at 20°C before injection into the HPLC. The commercial standards used were as follows: adenosine (Sigma-Aldrich; A9251), ADP sodium salt (Sigma-Aldrich; A2754), AMP (Fluka; catalog number 1930), APS sodium salt (Sigma-Aldrich; A5508), ATP (Sigma-Aldrich; A-5394), PAP (Sigma-Aldrich; A5763), PAPS (Sigma-Aldrich; A1651), and S-(5'-adenosyl)-L-Met chloride (Sigma-Aldrich; A7007).

#### HPLC of Adenosine Derivatives

The analyses of adenosines was performed by reverse-phase HPLC on a Gemini-NX 5- $\mu$ m C18 110A column (Phenomenex) connected to Waters 600E HPLC system and Waters 474 fluorescent detector (Waters). The gradient for separation of PAP was optimized as follows: equilibration of column for 0.2 min with 95% (v/v) of buffer A (5.7 mM [CH<sub>3</sub>(CH<sub>2</sub>)<sub>3</sub>]<sub>4</sub>N HSO<sub>4</sub> and 30.5 mM KH<sub>2</sub>PO<sub>4</sub>, pH 5.8) and 5% (v/v) buffer B (67% [v/v] acetonitrile and 33% [v/v] buffer A), linear gradient for 53 min up to 50% (v/v) of buffer B, and re-equilibration for 7 min with 5% (v/v) buffer B. Chromatograms were recorded and processed with the Milenium32 software (Waters) and edited using Adobe Illustrator (Adobe).

### Analysis of IPs

#### Feeding of Arabidopsis Seedlings with Radiolabeled myo-Inositol

Seeds were stratified and sown on 0.5 $\times$  MS agar containing vitamins (Duchefa Biochemie) and germinated at 22°C in a Sanyo light cabinet under long-day (16 h light/8 h dark) conditions at a fluence rate of 120  $\mu$ mol m<sup>-2</sup> s<sup>-1</sup> for 10 d. Five or six seedlings were subsequently placed in 0.4 mL of 0.5 $\times$  MS agar basal salts (Duchefa) liquid media to which 1.11 mBq of myo-[2-<sup>3</sup>H]inositol (specific activity 752 GBq/mmol; PerkinElmer) and 0.1 mM unlabeled myo-inositol were added. Seedlings were labeled for 72 h. Seedlings were washed briefly in water, blotted dry, transferred to a conical Eppendorf tube, frozen in liquid N<sub>2</sub>, and ground with a plastic pestle. The sample was extracted, with further grinding, with 0.3 mL of 0.6 M HCl after addition of 10  $\mu$ L of 1 mM phytic acid (Sigma-Aldrich; P8810) and left on ice for 30 min before centrifugation at 17,000g for 15 min at 4°C. The supernatant was diluted to 1 mL with water and applied directly to HPLC.

#### HPLC of IPs

IP extracts were analyzed on a 25 cm  $\times$  4.6-mm Partisphere SAX HPLC column (Whatman) with guard cartridge of the same material. Samples,

1 mL, were loaded and eluted with a gradient of phosphate, generated by mixing solvents from buffer reservoirs, A, water; B, 1.25 M  $\text{NH}_4\text{H}_2\text{PO}_4$ , adjusted to pH 3.35 with  $\text{H}_3\text{PO}_4$ , according to the following schedule: time (min), % B; 0,0; 5,0; 65,100; 75,100. Radioactivity was estimated in a Canberra Packard A515 detector fitted with a 0.5-mL flow cell after admixture of Optima Flo AP scintillation fluid (Canberra Packard) at a flow rate of 2 mL  $\text{min}^{-1}$ . The integration interval was 0.2 min. Data were exported from the Flo-One software (Canberra Packard) as ASCII files and redrawn in Delta Graph 4.0 (DeltaPoint).

### Feeding of *Arabidopsis* Seedlings with PAP

Seven-day-old, plate-grown Col-0 seedlings were incubated with 100  $\mu\text{L}$  of 0, 0.5, 1.0, and 2.0 mM PAP in 96-well plates. They were then incubated at LL (150  $\mu\text{mol m}^{-2} \text{s}^{-1}$ ) or HL (1500  $\mu\text{mol m}^{-2} \text{s}^{-1}$ ) for 50 min. After treatment, 1 mM luciferin was added and light emitted acquired overnight in a luminometer (FLUOStar OPTIMA).

### $\text{H}_2\text{O}_2$ Detection and Quantification

Foliar  $\text{H}_2\text{O}_2$  levels were visualized by 3,3'-diaminobenzidine (DAB) staining. Five-week-old plants grown hydroponically were transferred to a solution containing 25 mM DAB and incubated 1 h under HL (1000  $\mu\text{mol photons m}^{-2} \text{s}^{-1}$ ). The leaves were then placed into ethanol to remove the chlorophyll and the presence of  $\text{H}_2\text{O}_2$  visualized as a brown stain. Alternatively, leaf  $\text{H}_2\text{O}_2$  was quantified in 6-week-old, soil-grown plants with the Amplex Red Hydrogen Peroxide/Peroxidase Assay Kit (Invitrogen). Approximately 100 mg of leaf tissue was flash frozen in liquid nitrogen, ground, and extracted with 500  $\mu\text{L}$  of 20 mM  $\text{K}_2\text{HPO}_4$ , pH 6.5. The slurry was cleared by centrifugation at 16,000g for 15 min at 4°C. The supernatant was incubated with 0.1 mM Amplex Red reagent and 0.2 units  $\text{mL}^{-1}$  horseradish peroxidase at room temperature for 30 min in the dark (final reaction volume of 100  $\mu\text{L}$ ). Finally, absorbance was measured at 560 nm using a  $\mu\text{Quant}$  plate reader (BioTek Instruments) with Gen5 software, and the concentration of  $\text{H}_2\text{O}_2$  was calculated using a standard curve (0.5, 1, 2, and 5 mM  $\text{H}_2\text{O}_2$  range).

### Accession Numbers

Sequence data from this article can be found in the GenBank/EMBL data libraries under the following accession numbers: *ABI1* (At4g26080), *APX2* (At3g09640), *ATHB15* (At1g52150), *ATCYP5* (AT2G29960), *ELIP2* (At4g14690), *GNAT* (At2g39030), *MYB33* (At5g06100), *OST1* (At4g33950), *PHB* (At2g34710), *REV* (At5g60690), *SAL1/FRY1* (At5g63980), *SOT1* (At2g03760), *T5C23* (At4g11710), *VSP1* (At5g24780), *XRN2* (At5g42540), *XRN3* (At1g75660), and *XRN4* (At1g54490).

### Supplemental Data

The following materials are available in the online version of this article.

**Supplemental Figure 1.** PAP Feeding Experiments.

**Supplemental Figure 2.** The *sal1* Mutants *alx8* and *fry1-6* Lack SAL1 Protein and Have Similar Rosette Morphology.

**Supplemental Figure 3.** Inositol Phosphate Profile in Col-0 and the *sal1* Mutant *fry1-1*.

**Supplemental Figure 4.** Development of a Highly Sensitive Technique for Quantification of Phosphonucleotides.

**Supplemental Figure 5.** PAP, but Not PAPS, Accumulates in the *fou8* Mutants.

**Supplemental Figure 6.** Development of a New Method for Simultaneous Isolation of Cytosolic and Chloroplastic Fractions.

**Supplemental Figure 7.** Accumulation of 3' Cleavage Products in SAL1 Mutants.

**Supplemental Figure 8.** Antagonistic Changes in Global Gene Expression in *alx8*, *xrn4*, and *xrn2 xrn3*.

**Supplemental Table 1.** miRNA Targets Upregulated in *alx8*.

**Supplemental Table 2.** Genes Showing Similar Transcriptional Responses in Both *alx8* and *xrn2 xrn3* Mutants.

**Supplemental Table 3.** List of Primers.

**Supplemental Data Set 1.** Microarray Data for *alx8*, *xrn2 xrn3*, and *xrn4* Mutants.

### ACKNOWLEDGMENTS

We thank Albrecht G. von Arnim (University of Tennessee) for providing seeds of *fry1-6* (SALK\_020882) overexpressing a truncated form of SAL1 and *xrn2 xrn3* double mutants. Seeds of *fou8* and *fou8*-complemented line were kindly provided by Edward Farmer (University of Lausanne). We thank Hayley Whitfield (Brearley lab) for plant care and technical assistance. Funding to Australian researchers was provided by the Australian Research Council Centre of Excellence in Plant Energy Biology (CE0561495).

### AUTHOR CONTRIBUTIONS

G.M.E. performed cell fractionation and localization, adenosine derivative quantification, gene expression of complemented lines for the RT-PCR versus PAP correlations, immunoblots, and drought experiments. G.M.E. and B.J.P. planned and coordinated the experimental work, analyzed data, and wrote the article. P.A.C. screened and characterized *fry1-6: trSAL1* and *xrn* mutant lines, including drought testing, performed gene expression analyses, and assisted with PAP quantification and writing the article. W.P. performed the feeding experiments with PAP, DAB staining, and  $\text{H}_2\text{O}_2$  quantification. M.W. and R.H. developed the HPLC procedure to quantify PAP and also performed metabolite quantification. D.C. standardized the HPLC technique at Australian National University and helped to quantify PAP in chloroplastic fractions. C.C., E.G., and J.W. carried out the GFP fusion and microarray analyses. P.D., H.J., and E.M. prepared the pSAL1:SAL1:GFP construct, transformed the plants, and performed localization studies of the SAL1:GFP reporter gene in vivo. C.B. quantified the IPs in seedlings and seeds of different genotypes. All the authors discussed the results and commented on the article.

Received September 2, 2011; revised October 18, 2011; accepted November 10, 2011; published November 29, 2011.

### REFERENCES

- Albrecht, V., Simková, K., Carrie, C., Delannoy, E., Giraud, E., Whelan, J., Small, I.D., Apel, K., Badger, M.R., and Pogson, B.J. (2010). The cytoskeleton and the peroxisomal-targeted snowy cotyledon3 protein are required for chloroplast development in *Arabidopsis*. *Plant Cell* **22**: 3423–3438.
- Allison, D.B., Cui, X., Page, G.P., and Sabripour, M. (2006). Microarray data analysis: From disarray to consolidation and consensus. *Nat. Rev. Genet.* **7**: 55–65.
- Aronsson, H., and Jarvis, P. (2002). A simple method for isolating import-competent *Arabidopsis* chloroplasts. *FEBS Lett.* **529**: 215–220.

- Baldi, P., and Long, A.D.** (2001). A Bayesian framework for the analysis of microarray expression data: Regularized *t*-test and statistical inferences of gene changes. *Bioinformatics* **17**: 509–519.
- Ball, L., Accotto, G.-P., Bechtold, U., Creissen, G., Funck, D., Jimenez, A., Kular, B., Leyland, N., Mejia-Carranza, J., Reynolds, H., Karpinski, S., and Mullineaux, P.M.** (2004). Evidence for a direct link between glutathione biosynthesis and stress defense gene expression in *Arabidopsis*. *Plant Cell* **16**: 2448–2462.
- Bradbeer, J.W., Atkinson, Y.E., Borner, T., and Hagemann, R.** (1979). Cytoplasmic synthesis of plastid polypeptides may be controlled by plastid-synthesized RNA. *Nature* **279**: 816–817.
- Bürstenbinder, K., Rzewuski, G., Wirtz, M., Hell, R., and Sauter, M.** (2007). The role of methionine recycling for ethylene synthesis in *Arabidopsis*. *Plant J.* **49**: 238–249.
- Carrie, C., Murcha, M.W., Millar, A.H., Smith, S.M., and Whelan, J.** (2007). Nine 3-ketoacyl-CoA thiolases (KATs) and acetoacetyl-CoA thiolases (ACATs) encoded by five genes in *Arabidopsis thaliana* are targeted either to peroxisomes or cytosol but not to mitochondria. *Plant Mol. Biol.* **63**: 97–108.
- Carrie, C., Kühn, K., Murcha, M.W., Duncan, O., Small, I.D., O'Toole, N., and Whelan, J.** (2009). Approaches to defining dual-targeted proteins in *Arabidopsis*. *Plant J.* **57**: 1128–1139.
- Chen, H.A.O., and Xiong, L.** (2010). The bifunctional abiotic stress signalling regulator and endogenous RNA silencing suppressor FIERY1 is required for lateral root formation. *Plant Cell Environ.* **33**: 2180–2190.
- Clifton, R., Lister, R., Parker, K.L., Sapli, P.G., Elhafez, D., Millar, A.H., Day, D.A., and Whelan, J.** (2005). Stress-induced co-expression of alternative respiratory chain components in *Arabidopsis thaliana*. *Plant Mol. Biol.* **58**: 193–212.
- Dichtl, B., Stevens, A., and Tollervey, D.** (1997). Lithium toxicity in yeast is due to the inhibition of RNA processing enzymes. *EMBO J.* **16**: 7184–7195.
- Eubel, H., Lee, C.P., Kuo, J., Meyer, E.H., Taylor, N.L., and Millar, A.H.** (2007). Free-flow electrophoresis for purification of plant mitochondria by surface charge. *Plant J.* **52**: 583–594.
- Foyer, C.H., and Noctor, G.** (2009). Redox regulation in photosynthetic organisms: Signaling, acclimation, and practical implications. *Antioxid. Redox Signal.* **11**: 861–905.
- Fryer, M.J., Ball, L., Oxborough, K., Karpinski, S., Mullineaux, P.M., and Baker, N.R.** (2003). Control of Ascorbate Peroxidase 2 expression by hydrogen peroxide and leaf water status during excess light stress reveals a functional organisation of *Arabidopsis* leaves. *Plant J.* **33**: 691–705.
- Galvez-Valdivieso, G., Fryer, M.J., Lawson, T., Slattery, K., Truman, W., Smirnov, N., Asami, T., Davies, W.J., Jones, A.M., Baker, N.R., and Mullineaux, P.M.** (2009). The high light response in *Arabidopsis* involves ABA signaling between vascular and bundle sheath cells. *Plant Cell* **21**: 2143–2162.
- Gardeström, P., and Wigge, B.** (1988). Influence of photorespiration on ATP/ADP ratios in the chloroplasts, mitochondria, and cytosol, studied by rapid fractionation of barley (*Hordeum vulgare*) protoplasts. *Plant Physiol.* **88**: 69–76.
- Garmier, M., Carroll, A.J., Delannoy, E., Vallet, C., Day, D.A., Small, I.D., and Millar, A.H.** (2008). Complex I dysfunction redirects cellular and mitochondrial metabolism in *Arabidopsis*. *Plant Physiol.* **148**: 1324–1341.
- German, M.A., et al.** (2008). Global identification of microRNA-target RNA pairs by parallel analysis of RNA ends. *Nat. Biotechnol.* **26**: 941–946.
- Gil-Mascarell, R., López-Coronado, J.M., Bellés, J.M., Serrano, R., and Rodríguez, P.L.** (1999). The *Arabidopsis* HAL2-like gene family includes a novel sodium-sensitive phosphatase. *Plant J.* **17**: 373–383.
- Giraud, E., Ho, L.H., Clifton, R., Carroll, A., Estavillo, G., Tan, Y.F., Howell, K.A., Ivanova, A., Pogson, B.J., Millar, A.H., and Whelan, J.** (2008). The absence of ALTERNATIVE OXIDASE1a in *Arabidopsis* results in acute sensitivity to combined light and drought stress. *Plant Physiol.* **147**: 595–610.
- Gregory, B.D., O'Malley, R.C., Lister, R., Urlich, M.A., Tonti-Filippini, J., Chen, H., Millar, A.H., and Ecker, J.R.** (2008). A link between RNA metabolism and silencing affecting *Arabidopsis* development. *Dev. Cell* **14**: 854–866.
- Gy, I., Gascoli, V., Lauressergues, D., Morel, J.-B., Gombert, J., Proux, F., Proux, C., Vaucheret, H., and Mallory, A.C.** (2007). *Arabidopsis* FIERY1, XRN2, and XRN3 are endogenous RNA silencing suppressors. *Plant Cell* **19**: 3451–3461.
- Harari-Steinberg, O., Ohad, I., and Chamovitz, D.A.** (2001). Dissection of the light signal transduction pathways regulating the two early light-induced protein genes in *Arabidopsis*. *Plant Physiol.* **127**: 986–997.
- Hirsch, J., et al.** (2011). A novel *frt1* allele reveals the existence of a mutant phenotype unrelated to 5'→3' exoribonuclease (XRN) activities in *Arabidopsis thaliana* roots. *PLoS ONE* **6**: e16724.
- Hruz, T., Laule, O., Szabo, G., Wessendorp, F., Bleuler, S., Oertle, L., Widmayer, P., Gruissem, W., and Zimmermann, P.** (2008). Genevestigator V3: A reference expression database for the meta-analysis of transcriptomes. *Adv. Bioinformatics* **2008**: 420747.
- Karpinski, S., Escobar, C., Karpinska, B., Creissen, G., and Mullineaux, P.M.** (1997). Photosynthetic electron transport regulates the expression of cytosolic ascorbate peroxidase genes in *Arabidopsis* during excess light stress. *Plant Cell* **9**: 627–640.
- Karpinski, S., Reynolds, H., Karpinska, B., Wingsle, G., Creissen, G., and Mullineaux, P.** (1999). Systemic signaling and acclimation in response to excess excitation energy in *Arabidopsis*. *Science* **284**: 654–657.
- Kastenmayer, J.P., and Green, P.J.** (2000). Novel features of the XRN-family in *Arabidopsis*: Evidence that AtXRN4, one of several orthologs of nuclear Xrn2p/Rat1p, functions in the cytoplasm. *Proc. Natl. Acad. Sci. USA* **97**: 13985–13990.
- Kim, B.H., and von Arnim, A.G.** (2009). FIERY1 regulates light-mediated repression of cell elongation and flowering time via its 3'(2'),5'-bisphosphate nucleotidase activity. *Plant J.* **58**: 208–219.
- Kim, M., Krogan, N.J., Vasiljeva, L., Rando, O.J., Nede, E., Greenblatt, J.F., and Buratowski, S.** (2004). The yeast Rat1 exonuclease promotes transcription termination by RNA polymerase II. *Nature* **432**: 517–522.
- Kimura, M., Manabe, K., Abe, T., Yoshida, S., Matsui, M., and Yamamoto, Y.Y.** (2003). Analysis of hydrogen peroxide-independent expression of the high-light-inducible ELIP2 gene with the aid of the ELIP2 promoter-luciferase fusions. *Photochem. Photobiol.* **77**: 668–674.
- Kimura, M., Yamamoto, Y., Seki, M., Sakurai, T., Sato, M., Shinozaki, K., Manabe, K., and Matsui, M.** (2002). Identification of *Arabidopsis* genes regulated by high light-stress using cDNA microarray. *Plant Cell Physiol.* **43**: S159.
- Kindgren, P., Eriksson, M.-J., Benedict, C., Mohapatra, A., Gough, S.P., Hansson, M., Kieselbach, T., and Strand, A.** (2011). A novel proteomic approach reveals a role for Mg-protoporphyrin IX in response to oxidative stress. *Physiol. Plant.* **141**: 310–320.
- Klein, M., and Papenbrock, J.** (2004). The multi-protein family of *Arabidopsis* sulphotransferases and their relatives in other plant species. *J. Exp. Bot.* **55**: 1809–1820.
- Kleine, T., Kindgren, P., Benedict, C., Hendrickson, L., and Strand, A.** (2007). Genome-wide gene expression analysis reveals a critical role for CRYPTOCHROME1 in the response of *Arabidopsis* to high irradiance. *Plant Physiol.* **144**: 1391–1406.
- Kleine, T., Voigt, C., and Leister, D.** (2009). Plastid signalling to the

- nucleus: Messengers still lost in the mists? *Trends Genet.* **25**: 185–192.
- Koussevitzky, S., Nott, A., Mockler, T.C., Hong, F., Sachetto-Martins, G., Surpin, M., Lim, J., Mittler, R., and Chory, J.** (2007). Signals from chloroplasts converge to regulate nuclear gene expression. *Science* **316**: 715–719.
- Larkin, R.M., Alonso, J.M., Ecker, J.R., and Chory, J.** (2003). GUN4, a regulator of chlorophyll synthesis and intracellular signaling. *Science* **299**: 902–906.
- Lee, K.P., Kim, C., Landgraf, F., and Apel, K.** (2007). EXECUTER1- and EXECUTER2-dependent transfer of stress-related signals from the plastid to the nucleus of *Arabidopsis thaliana*. *Proc. Natl. Acad. Sci. USA* **104**: 10270–10275.
- Leonhardt, N., Kwak, J.M., Robert, N., Waner, D., Leonhardt, G., and Schroeder, J.I.** (2004). Microarray expression analyses of *Arabidopsis* guard cells and isolation of a recessive abscisic acid hypersensitive protein phosphatase 2C mutant. *Plant Cell* **16**: 596–615.
- Logemann, E., Birkenbihl, R.P., Ulker, B., and Somssich, I.E.** (2006). An improved method for preparing *Agrobacterium* cells that simplifies the *Arabidopsis* transformation protocol. *Plant Methods* **2**: 16.
- Millar, A.H., Carrie, C., Pogson, B., and Whelan, J.** (2009). Exploring the function-location nexus: Using multiple lines of evidence in defining the subcellular location of plant proteins. *Plant Cell* **21**: 1625–1631.
- Mochizuki, N., Tanaka, R., Tanaka, A., Masuda, T., and Nagatani, A.** (2008). The steady-state level of Mg-protoporphyrin IX is not a determinant of plastid-to-nucleus signaling in *Arabidopsis*. *Proc. Natl. Acad. Sci. USA* **105**: 15184–15189.
- Moulin, M., McCormac, A.C., Terry, M.J., and Smith, A.G.** (2008). Tetrapyrrole profiling in *Arabidopsis* seedlings reveals that retrograde plastid nuclear signaling is not due to Mg-protoporphyrin IX accumulation. *Proc. Natl. Acad. Sci. USA* **105**: 15178–15183.
- Mugford, S.G., et al.** (2009). Disruption of adenosine-5'-phosphosulfate kinase in *Arabidopsis* reduces levels of sulfated secondary metabolites. *Plant Cell* **21**: 910–927.
- Murcha, M.W., Elhafez, D., Lister, R., Tonti-Filippini, J., Baumgartner, M., Philippar, K., Carrie, C., Mokranjac, D., Soll, J., and Whelan, J.** (2007). Characterization of the preprotein and amino acid transporter gene family in *Arabidopsis*. *Plant Physiol.* **143**: 199–212.
- Murguía, J.R., Bellés, J.M., and Serrano, R.** (1996). The yeast HAL2 nucleotidase is an in vivo target of salt toxicity. *J. Biol. Chem.* **271**: 29029–29033.
- Nakagawa, T., Kurose, T., Hino, T., Tanaka, K., Kawamukai, M., Niwa, Y., Toyooka, K., Matsuoka, K., Jinbo, T., and Kimura, T.** (2007). Development of series of gateway binary vectors, pGWBs, for realizing efficient construction of fusion genes for plant transformation. *J. Biosci. Bioeng.* **104**: 34–41.
- Nott, A., Jung, H.-S., Koussevitzky, S., and Chory, J.** (2006). Plastid-to-nucleus retrograde signaling. *Annu. Rev. Plant Biol.* **57**: 739–759.
- Olinares, P.D.B., Ponnala, L., and van Wijk, K.J.** (2010). Megadalton complexes in the chloroplast stroma of *Arabidopsis thaliana* characterized by size exclusion chromatography, mass spectrometry, and hierarchical clustering. *Mol. Cell. Proteomics* **9**: 1594–1615.
- Olmedo, G., Guo, H., Gregory, B.D., Nourizadeh, S.D., Aguilar-Henonin, L., Li, H., An, F., Guzman, P., and Ecker, J.R.** (2006). ETHYLENE-INSENSITIVE5 encodes a 5'→3' exonuclease required for regulation of the EIN3-targeting F-box proteins EBF1/2. *Proc. Natl. Acad. Sci. USA* **103**: 13286–13293.
- Peltier, J.-B., Cai, Y., Sun, Q., Zabrouskov, V., Giacomelli, L., Rudella, A., Ytterberg, A.J., Rutschow, H., and van Wijk, K.J.** (2006). The oligomer stromal proteome of *Arabidopsis thaliana* chloroplasts. *Mol. Cell. Proteomics* **5**: 114–133.
- Perera, I.Y., Hung, C.-Y., Moore, C.D., Stevenson-Paulik, J., and Boss, W.F.** (2008). Transgenic *Arabidopsis* plants expressing the type 1 inositol 5-phosphatase exhibit increased drought tolerance and altered abscisic acid signaling. *Plant Cell* **20**: 2876–2893.
- Pfaffl, M.W.** (2001). A new mathematical model for relative quantification in real-time RT-PCR. *Nucleic Acids Res.* **29**: e45.
- Pfannschmidt, T.** (2010). Plastidial retrograde signalling—A true “plastid factor” or just metabolite signatures? *Trends Plant Sci.* **15**: 427–435.
- Pfannschmidt, T., Bräutigam, K., Wagner, R., Dietzel, L., Schröter, Y., Steiner, S., and Nykytenko, A.** (2009). Potential regulation of gene expression in photosynthetic cells by redox and energy state: Approaches towards better understanding. *Ann. Bot. (Lond.)* **103**: 599–607.
- Pogson, B.J., Woo, N.S., Förster, B., and Small, I.D.** (2008). Plastid signalling to the nucleus and beyond. *Trends Plant Sci.* **13**: 602–609.
- Quintero, F.J., Garcíadeblás, B., and Rodríguez-Navarro, A.** (1996). The SAL1 gene of *Arabidopsis*, encoding an enzyme with 3'(2'),5'-bisphosphate nucleotidase and inositol polyphosphate 1-phosphatase activities, increases salt tolerance in yeast. *Plant Cell* **8**: 529–537.
- Robles, P., Fleury, D., Candela, H., Cnops, G., Alonso-Peral, M.M., Anami, S., Falcone, A., Caldana, C., Willmitzer, L., Ponce, M.R., Van Lijsebettens, M., and Micol, J.L.** (2010). The RON1/FRY1/SAL1 gene is required for leaf morphogenesis and venation patterning in *Arabidopsis*. *Plant Physiol.* **152**: 1357–1372.
- Rodríguez, V.M., Chételat, A., Majcherczyk, P., and Farmer, E.E.** (2010). Chloroplastic phosphoadenosine phosphosulfate metabolism regulates basal levels of the prohormone jasmonic acid in *Arabidopsis* leaves. *Plant Physiol.* **152**: 1335–1345.
- Rossel, J.B., Walter, P.B., Hendrickson, L., Chow, W.S., Poole, A., Mullineaux, P.M., and Pogson, B.J.** (2006). A mutation affecting ASCORBATE PEROXIDASE 2 gene expression reveals a link between responses to high light and drought tolerance. *Plant Cell Environ.* **29**: 269–281.
- Rossel, J.B., Wilson, P.B., Hussain, D., Woo, N.S., Gordon, M.J., Mewett, O.P., Howell, K.A., Whelan, J., Kazan, K., and Pogson, B.J.** (2007). Systemic and intracellular responses to photooxidative stress in *Arabidopsis*. *Plant Cell* **19**: 4091–4110.
- Ruckle, M.E., DeMarco, S.M., and Larkin, R.M.** (2007). Plastid signals remodel light signaling networks and are essential for efficient chloroplast biogenesis in *Arabidopsis*. *Plant Cell* **19**: 3944–3960.
- Souret, F.F., Kastenmayer, J.P., and Green, P.J.** (2004). AtXRN4 degrades mRNA in *Arabidopsis* and its substrates include selected miRNA targets. *Mol. Cell* **15**: 173–183.
- Strand, A., Asami, T., Alonso, J., Ecker, J.R., and Chory, J.** (2003). Chloroplast to nucleus communication triggered by accumulation of Mg-protoporphyrin IX. *Nature* **421**: 79–83.
- Susek, R.E., Ausubel, F.M., and Chory, J.** (1993). Signal transduction mutants of *Arabidopsis* uncouple nuclear CAB and RBCS gene expression from chloroplast development. *Cell* **74**: 787–799.
- Thirkettle-Watts, D., McCabe, T.C., Clifton, R., Moore, C., Finnegan, P.M., Day, D.A., and Whelan, J.** (2003). Analysis of the alternative oxidase promoters from soybean. *Plant Physiol.* **133**: 1158–1169.
- Tognetti, V.B., et al.** (2010). Perturbation of indole-3-butyric acid homeostasis by the UDP-glucosyltransferase UGT74E2 modulates *Arabidopsis* architecture and water stress tolerance. *Plant Cell* **22**: 2660–2679.
- Van Breusegem, F., Bailey-Serres, J., and Mittler, R.** (2008). Unraveling the tapestry of networks involving reactive oxygen species in plants. *Plant Physiol.* **147**: 978–984.
- van Dijk, E.L., et al.** (2011). XUTs are a class of Xrn1-sensitive antisense regulatory non-coding RNA in yeast. *Nature* **475**: 114–117.
- Vranová, E., Inzé, D., and Van Breusegem, F.** (2002). Signal transduction during oxidative stress. *J. Exp. Bot.* **53**: 1227–1236.
- Wagner, D., Przybyla, D., Op den Camp, R., Kim, C., Landgraf, F., Lee, K.P., Würsch, M., Laloi, C., Nater, M., Hideg, E., and Apel, K.**

- (2004). The genetic basis of singlet oxygen-induced stress responses of *Arabidopsis thaliana*. *Science* **306**: 1183–1185.
- West, S., Gromak, N., and Proudfoot, N.J.** (2004). Human 5' → 3' exonuclease Xrn2 promotes transcription termination at co-transcriptional cleavage sites. *Nature* **432**: 522–525.
- Wilson, P.B., Estavillo, G.M., Field, K.J., Pornsiriwong, W., Carroll, A.J., Howell, K.A., Woo, N.S., Lake, J.A., Smith, S.M., Harvey Millar, A., von Caemmerer, S., and Pogson, B.J.** (2009). The nucleotidase/phosphatase SAL1 is a negative regulator of drought tolerance in *Arabidopsis*. *Plant J.* **58**: 299–317.
- Woo, N.S., Badger, M.R., and Pogson, B.J.** (2008). A rapid, non-invasive procedure for quantitative assessment of drought survival using chlorophyll fluorescence. *Plant Methods* **4**: 27.
- Woodson, J.D., Perez-Ruiz, J.M., and Chory, J.** (2011). Heme synthesis by plastid ferrochelatase I regulates nuclear gene expression in plants. *Curr. Biol.* **21**: 897–903.
- Xiong, L.M., Lee Bh, Ishitani, M., Lee, H., Zhang, C.Q., and Zhu, J.K.** (2001). FIERY1 encoding an inositol polyphosphate 1-phosphatase is a negative regulator of abscisic acid and stress signaling in *Arabidopsis*. *Genes Dev.* **15**: 1971–1984.
- Zakrzewska-Placzek, M., Souret, F.F., Sobczyk, G.J., Green, P.J., and Kufel, J.** (2010). *Arabidopsis thaliana* XRN2 is required for primary cleavage in the pre-ribosomal RNA. *Nucleic Acids Res.* **38**: 4487–4502.
- Zhang, J., et al.** (2011). Inositol trisphosphate-induced Ca<sup>2+</sup> signaling modulates auxin transport and PIN polarity. *Dev. Cell* **20**: 855–866.